Mean-field approximation and deformation

平均場近似＝2体場→1体場に近似

$$H = \sum_{i=1}^{A} -\frac{\hbar^2}{2m}\nabla_i^2 + \frac{1}{2}\sum_{i,j}^{A} v(\boldsymbol{r}_i, \boldsymbol{r}_j)$$

$$= \sum_{i=1}^{A}\left(-\frac{\hbar^2}{2m}\nabla_i^2 + V_{\rm MF}(\boldsymbol{r}_i)\right) + \frac{1}{2}\sum_{i,j}^{A} v(\boldsymbol{r}_i, \boldsymbol{r}_j) - \sum_i V_{\rm MF}(\boldsymbol{r}_i)$$

→ $\Psi_{\rm MF}$: ハミルトニアン H が持っている対称性を持たなくてもいい

"対称性の自発的破れ"

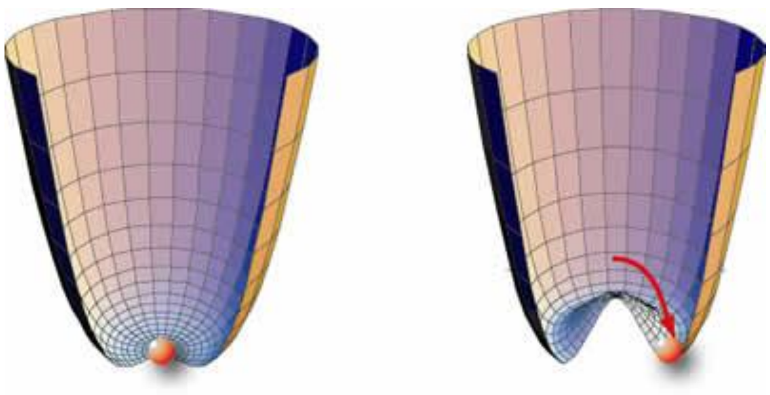

Ψ_{MF} ：ハミルトニアン H が持っている対称性を持たなくてもいい

典型的な例

➢ **並進対称性:** 原子核の平均場近似（DFT）では常に破れる

$$H = -\sum_{i=1}^{A}\frac{\hbar^2}{2m}\boldsymbol{\nabla}_i^2 + \frac{1}{2}\sum_{i,j} v(\boldsymbol{r}_i - \boldsymbol{r}_j) \rightarrow \sum_{i=1}^{A}\left(-\frac{\hbar^2}{2m}\boldsymbol{\nabla}_i^2 + \underline{\underline{V_{\mathrm{MF}}(\boldsymbol{r}_i)}}\right)$$

➢ **回転対称性**

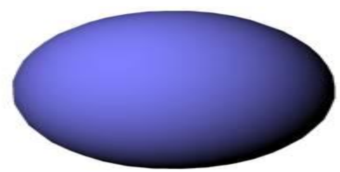

$\rightarrow V(r,\theta)$

変形した基底状態

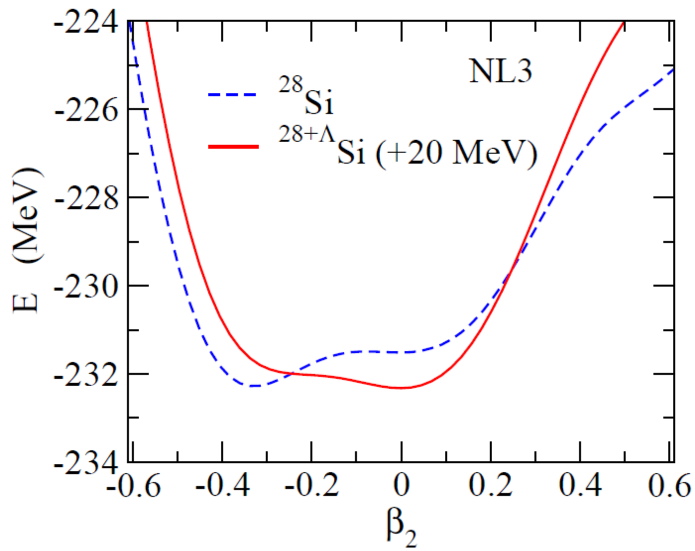

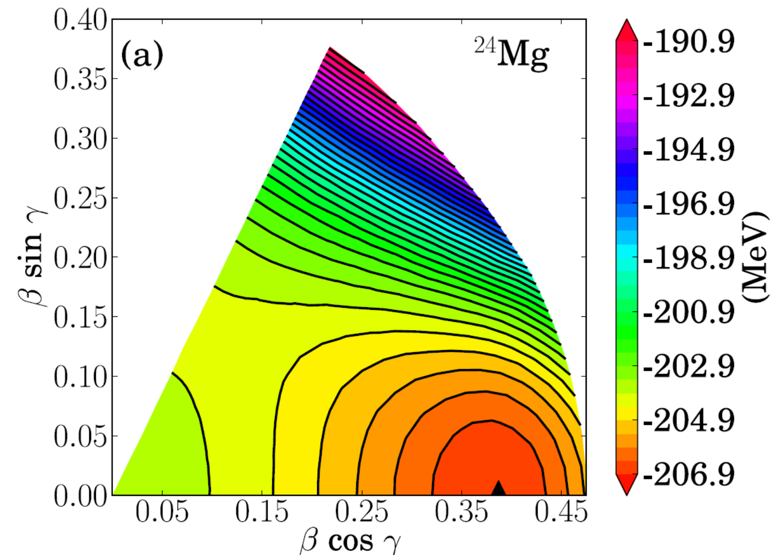

deformation and two-neutron separation energy

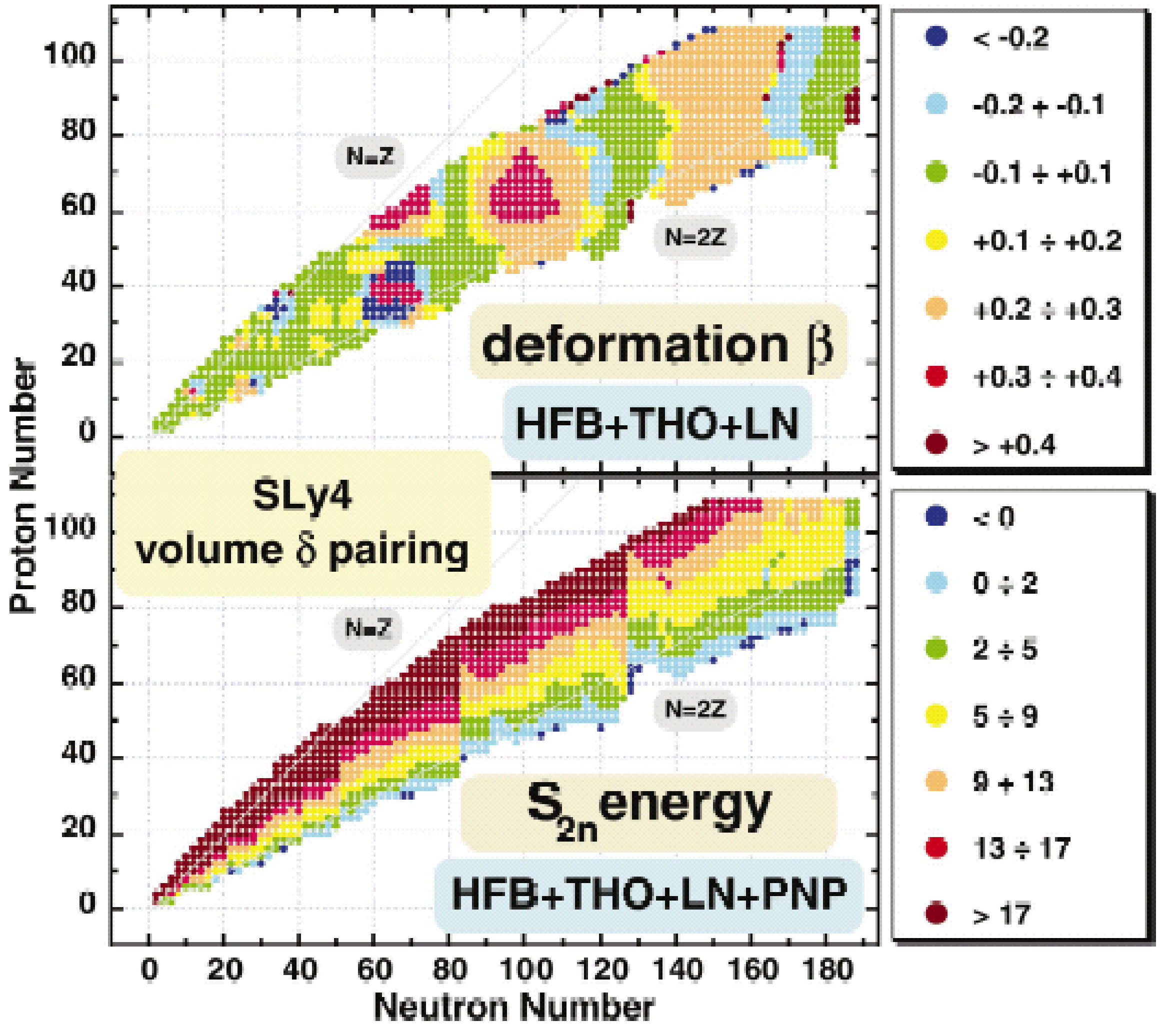

M.V. Stoitsov et al., PRC68('03)054312

Nuclear Deformation

核変形の実験的な証拠

Excitation spectra of ^{154}Sm

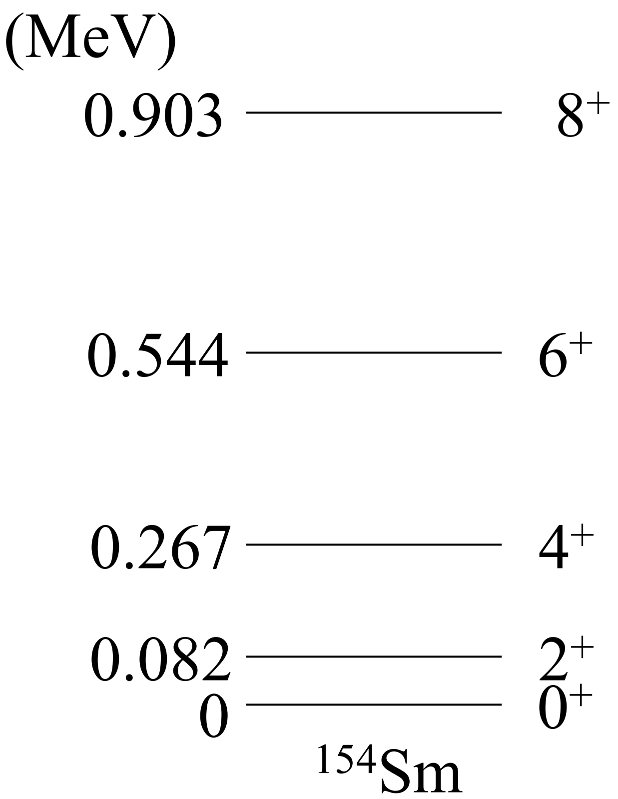

$$E_I \sim \frac{I(I+1)\hbar^2}{2\mathcal{J}}$$

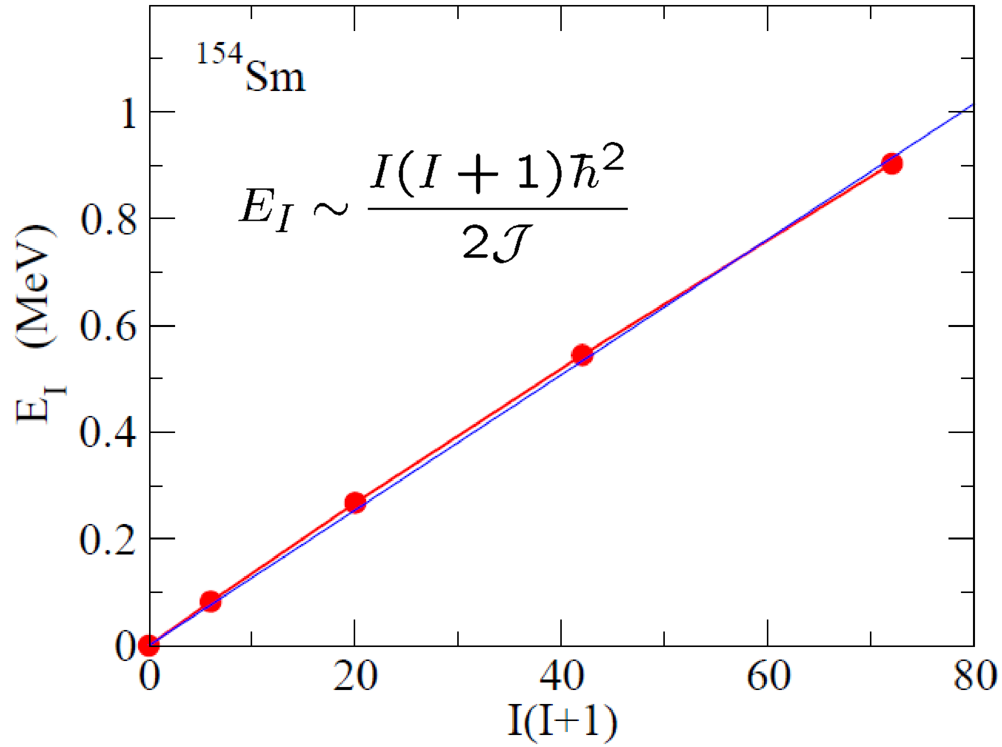

cf. a classical rigid rotor

$$E = \frac{1}{2}\mathcal{J}\omega^2 = \frac{I^2}{2\mathcal{J}}$$

$$(I = \mathcal{J}\omega, \;\; \omega = \dot{\theta})$$

^{154}Sm : a typical deformed nucleus

$$E_I \sim \frac{I(I+1)\hbar^2}{2\mathcal{J}}$$

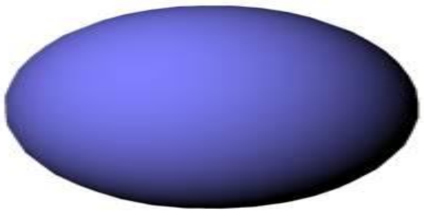

^{154}Sm

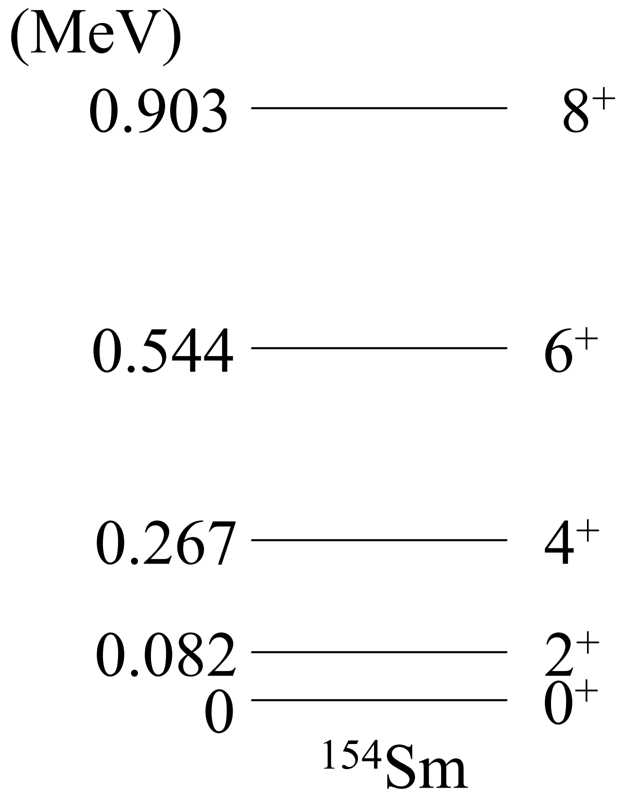

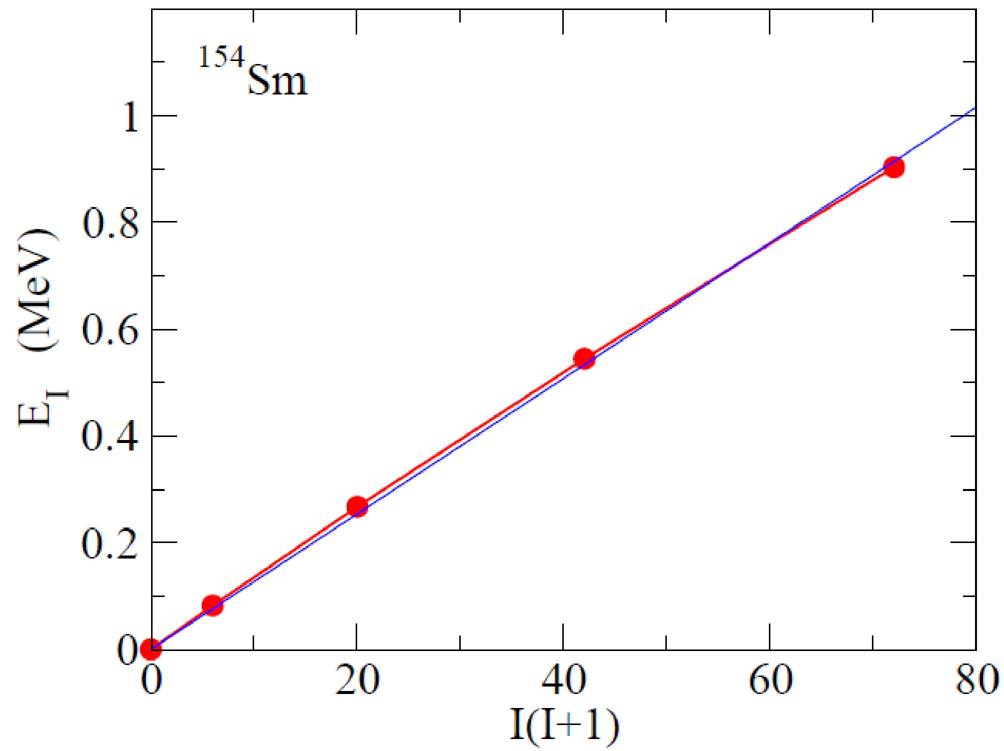

rotational spectrum

cf. a classical rigid rotor

$$E = \frac{1}{2}\mathcal{J}\omega^2 = \frac{I^2}{2\mathcal{J}}$$

$$(I = \mathcal{J}\omega,\ \ \omega = \dot{\theta})$$

One-particle motion in a deformed potential

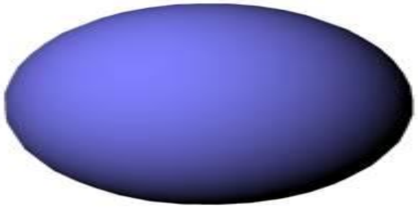

$\rightarrow V(r,\theta)$

$$\left[-\frac{\hbar^2}{2m}\nabla^2 + V(r,\theta) - E\right]\psi(\boldsymbol{r}) = 0$$

(note) $V(r,\theta)$ → 回転対称性を持っていない
→ 角運動量がいい量子数ではない

$$\psi_{nlm}(\boldsymbol{r}) = R_{nl}(r)Y_{lm}(\hat{\boldsymbol{r}}) \rightarrow \psi_{nK}(\boldsymbol{r}) = \sum_l R_{nl}(r)Y_{lK}(\hat{\boldsymbol{r}})$$

＊軸対称変形であれば l_z は保存

$$E_{nl} \rightarrow E_{nK}$$

（準備）1次元井戸型ポテンシャル

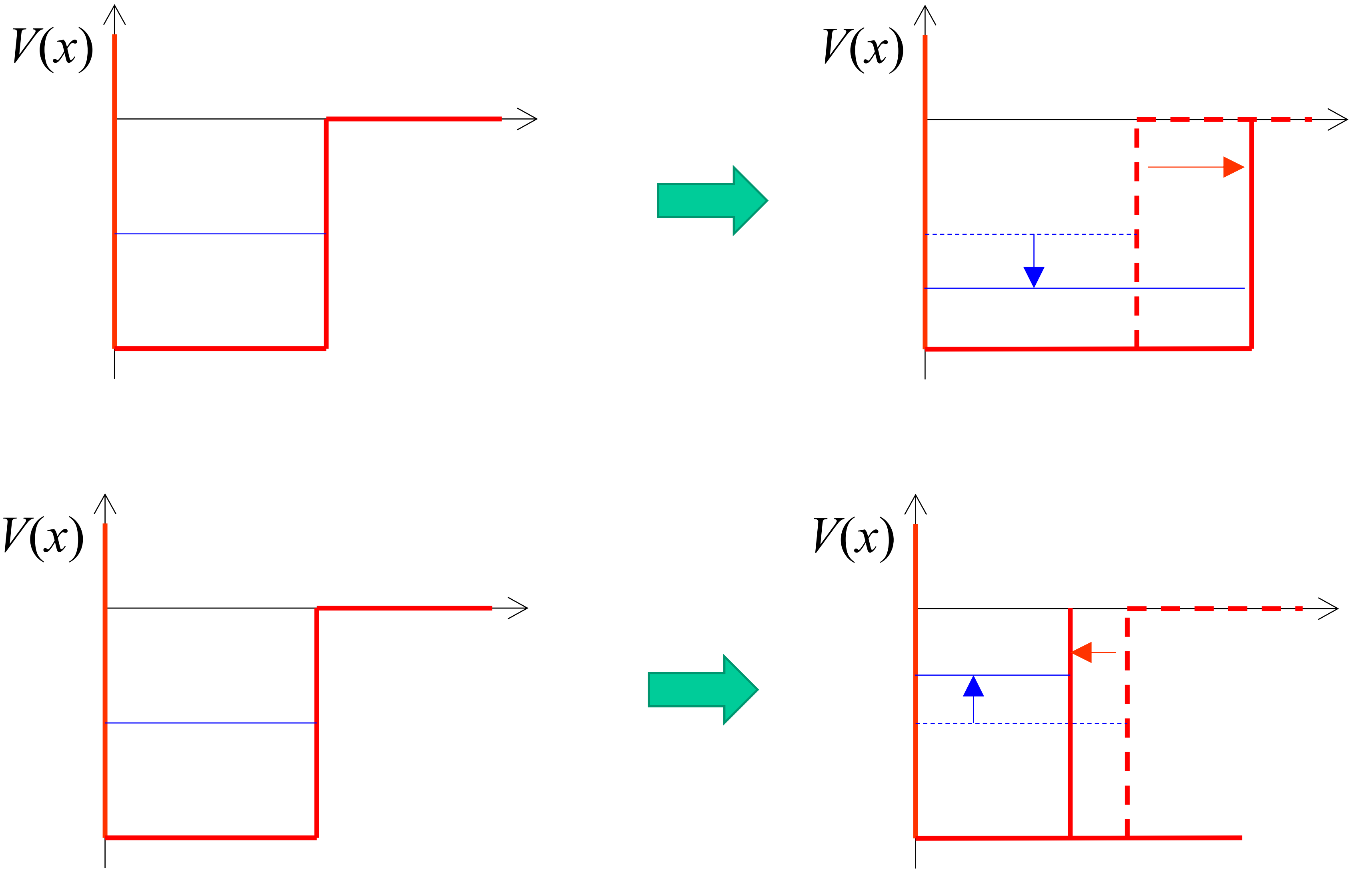

One-particle motion in a deformed potential

長軸に沿った運動

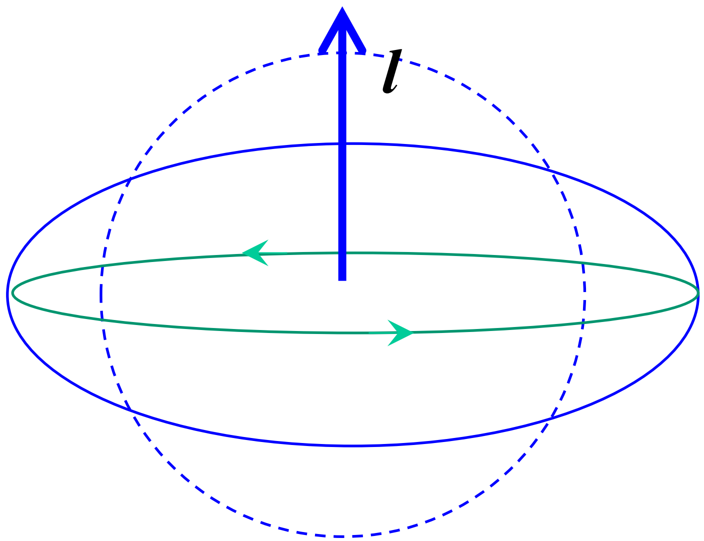

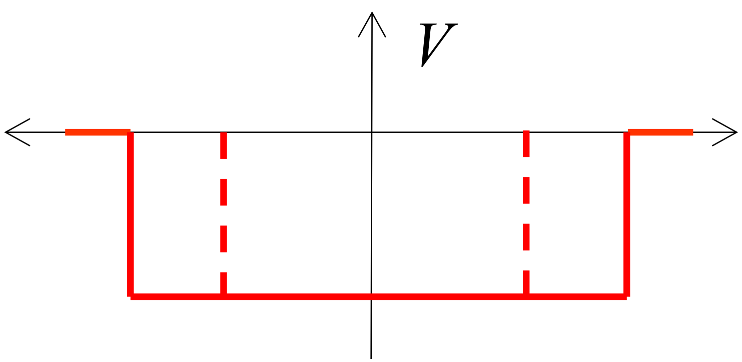

$E \rightarrow$ 小

短軸に沿った運動

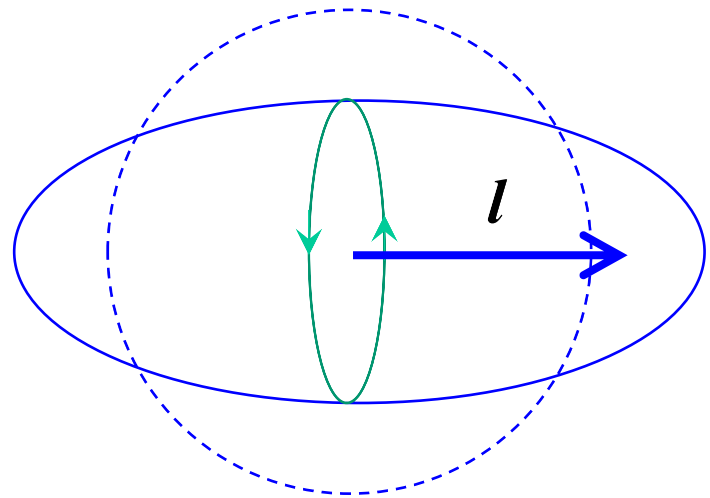

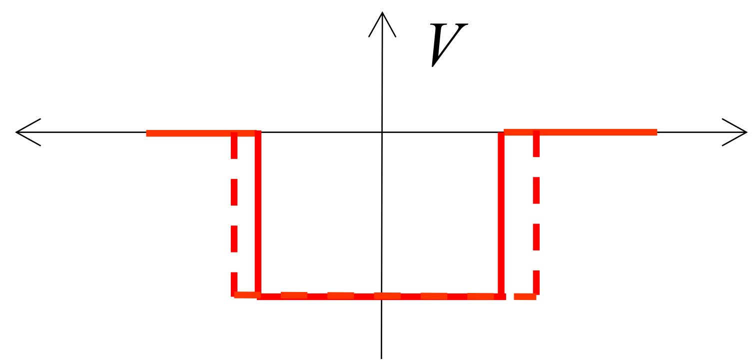

$E \rightarrow$ 大

One-particle motion in a deformed potential

長軸に沿った運動

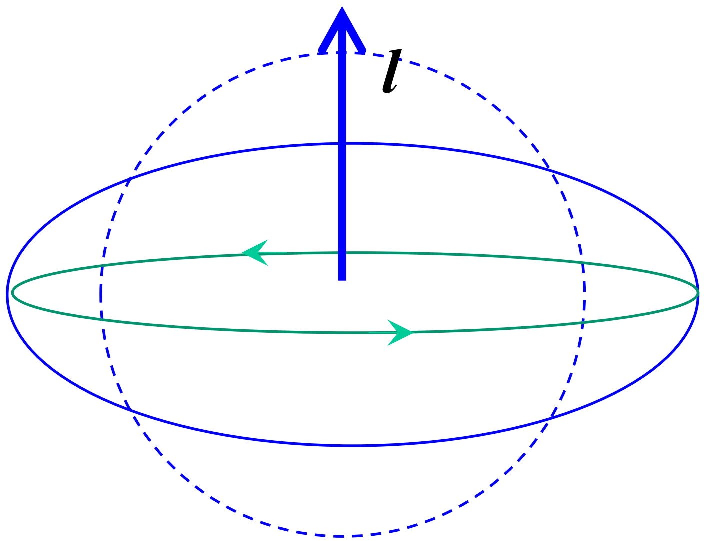

短軸に沿った運動

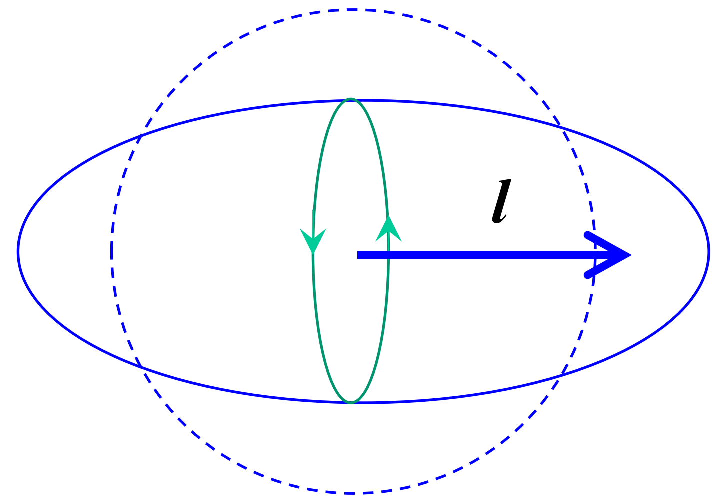

→ z軸

軌道が
スプリット

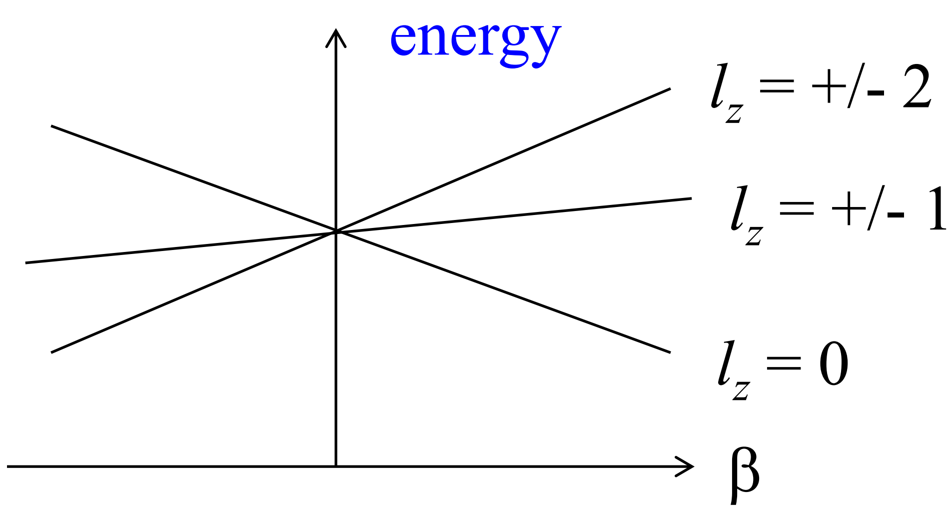

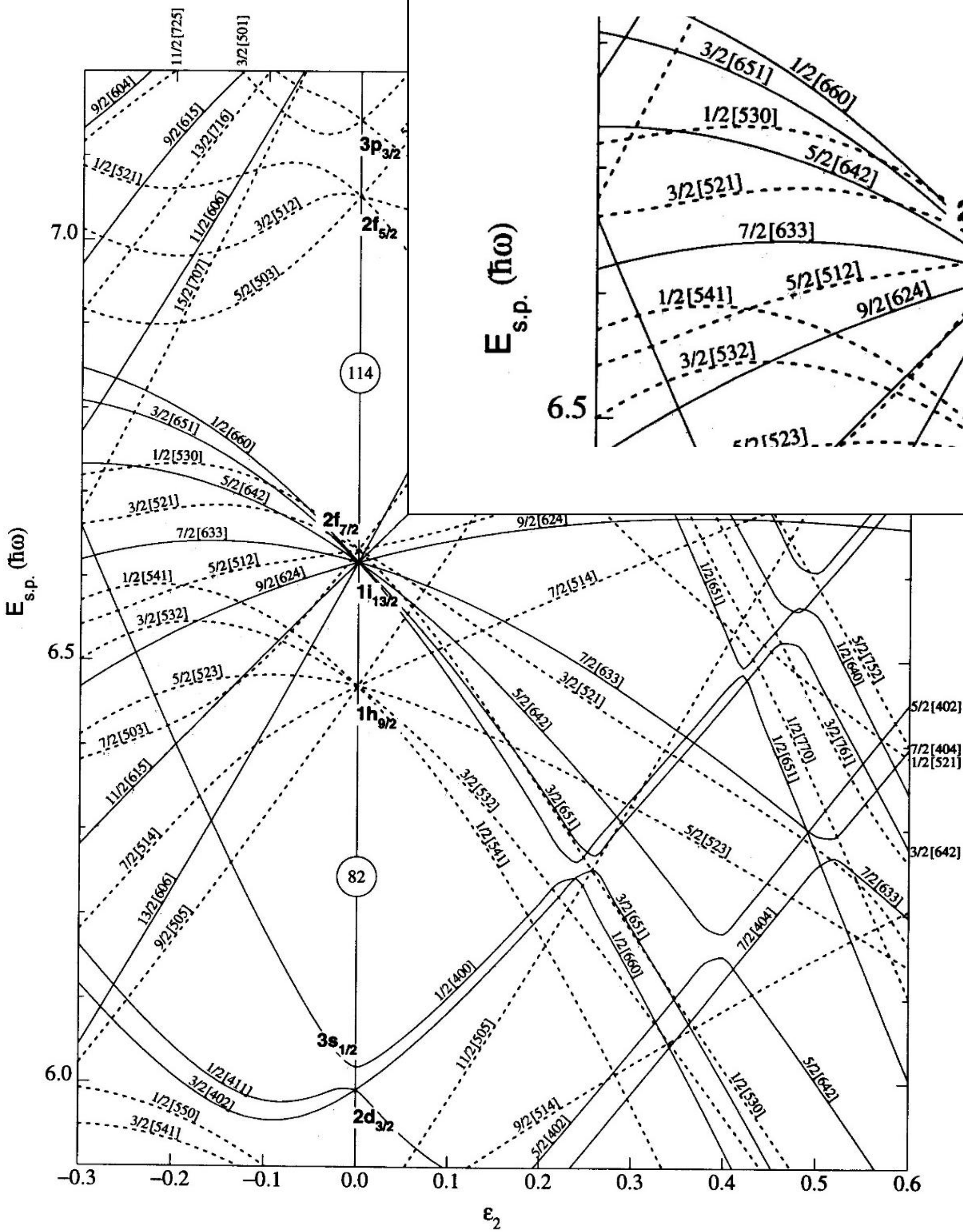

Figure 13. Nilsson diagram for protons, $Z \geq 82$ ($\varepsilon_4 = \varepsilon_2^2/6$).

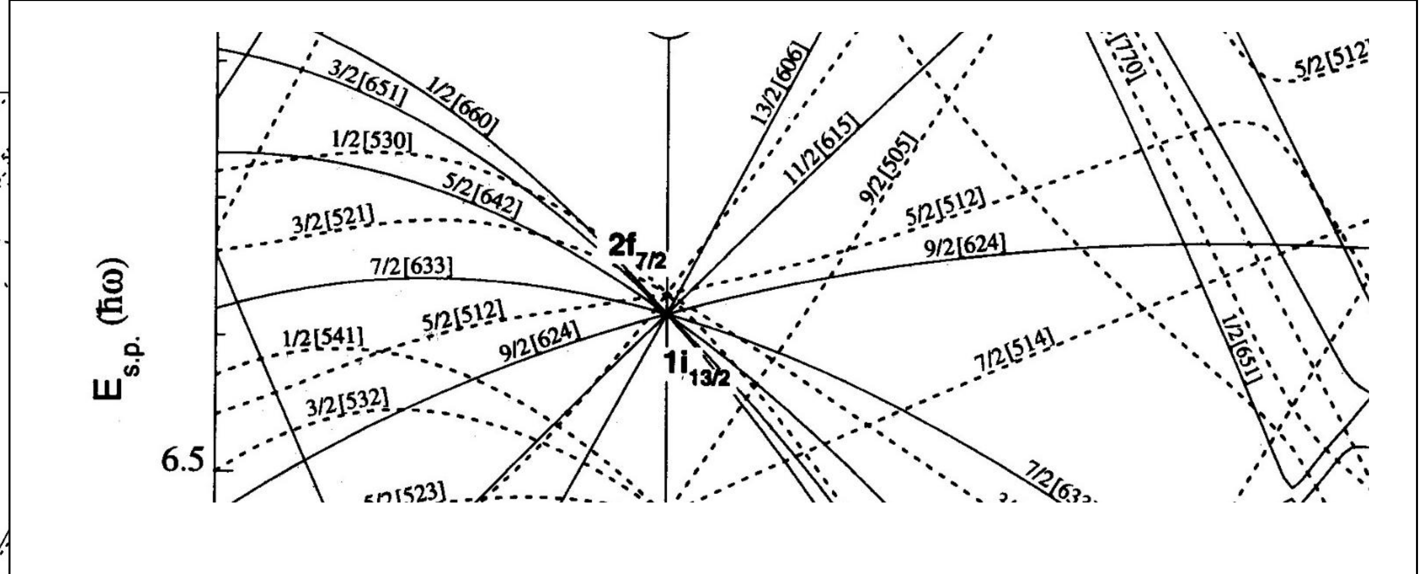

Nilsson diagram

$h = T + V(r,\theta)$
の固有値

原子核の変形と殻効果

液滴模型

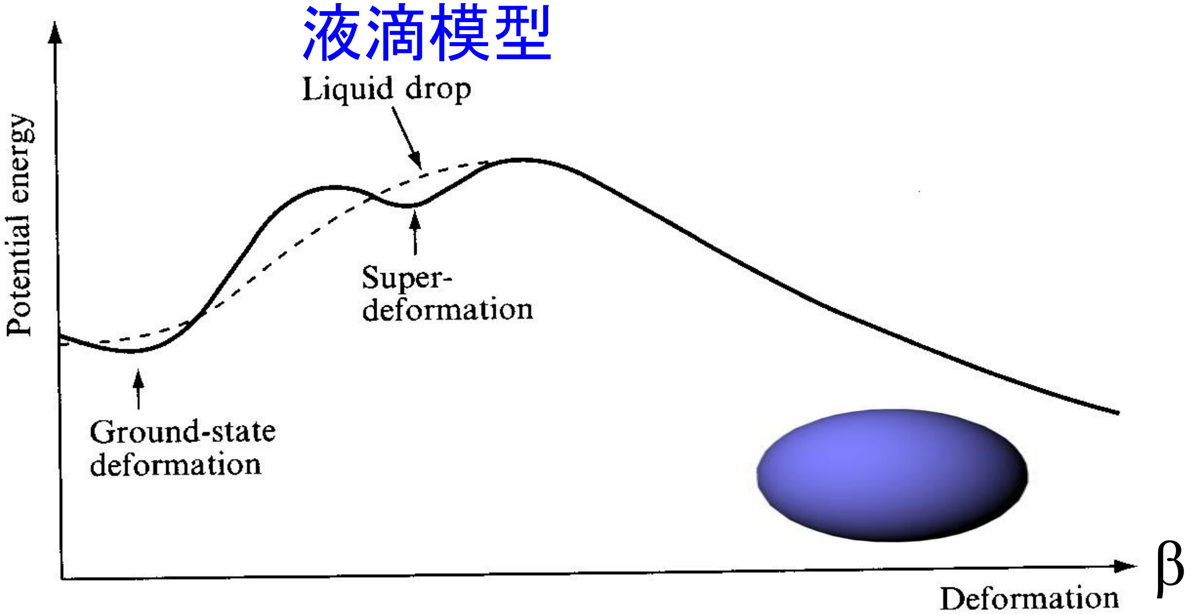

$$E(\beta) = E_{LDM}(\beta) + E_{\text{shell}}(\beta)$$

液滴模型→常に球形が基底状態

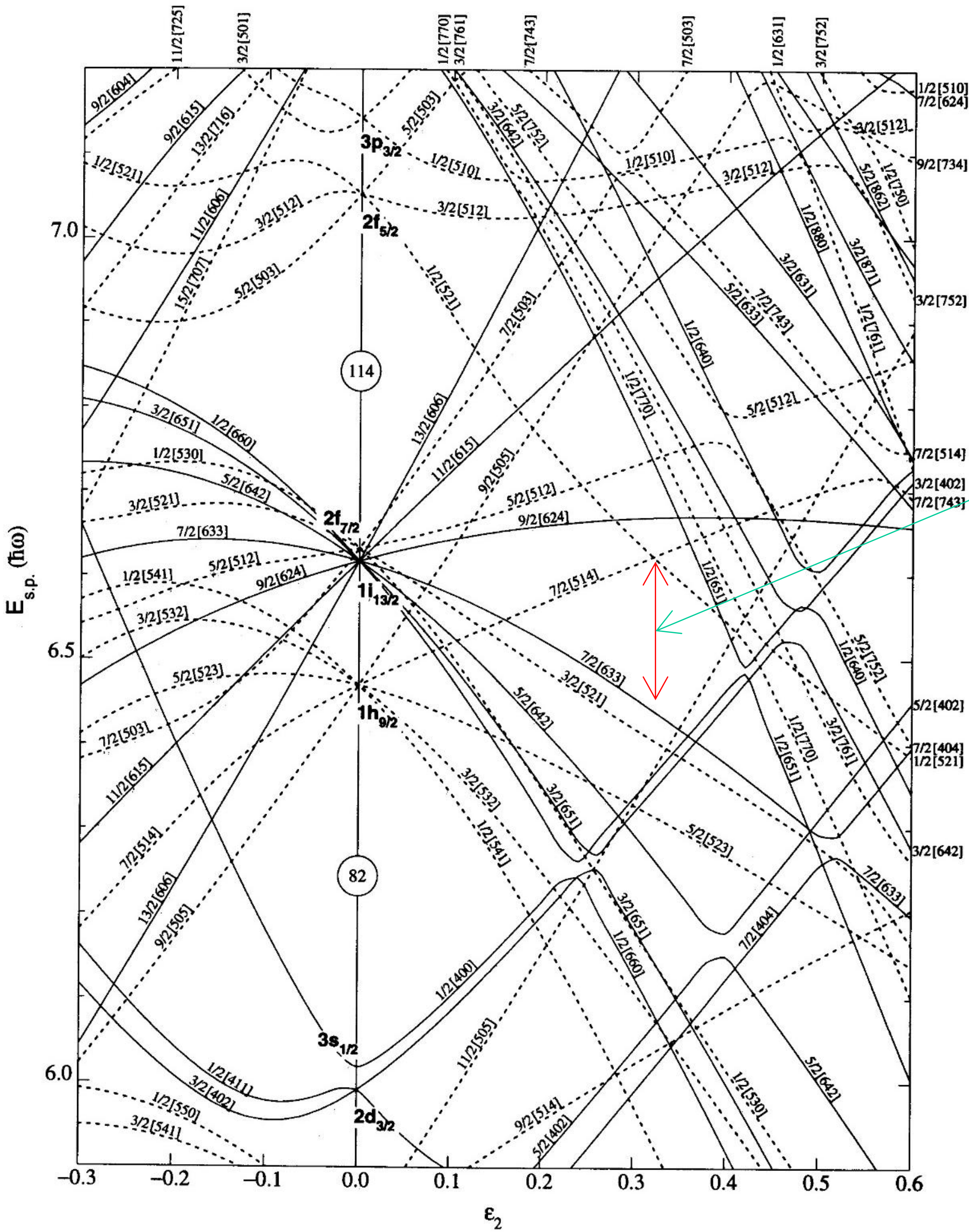

Figure 13. Nilsson diagram for protons, $Z \geq 82$ ($\varepsilon_4 = \varepsilon_2^2/6$).

変形することにより
ギャップが開く

Nilsson diagram

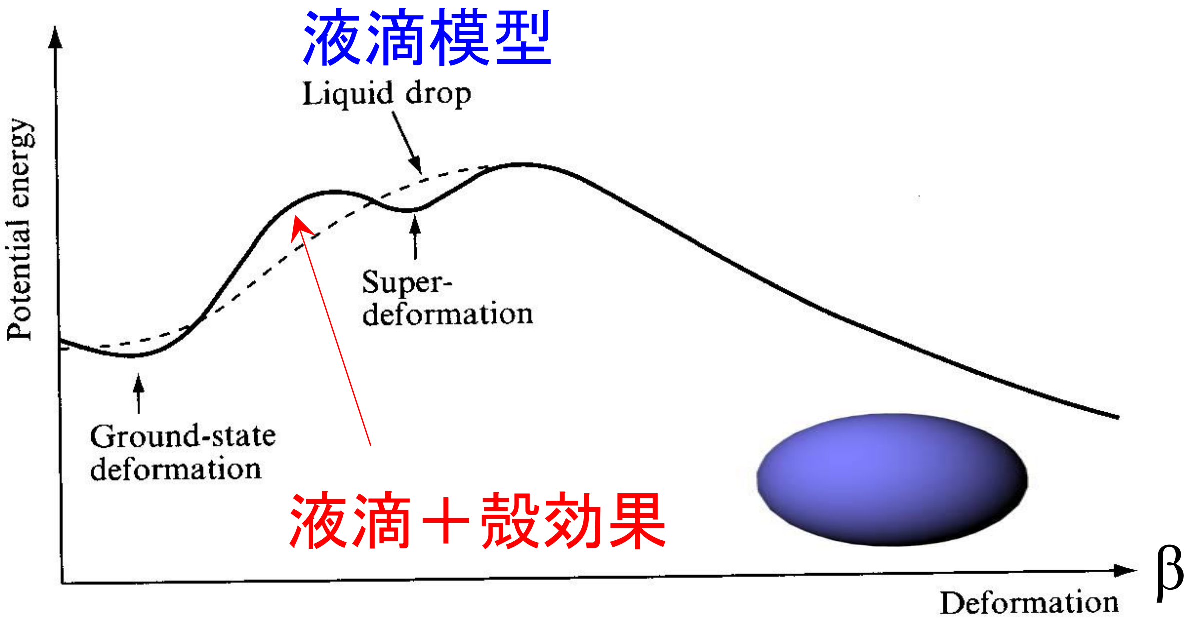

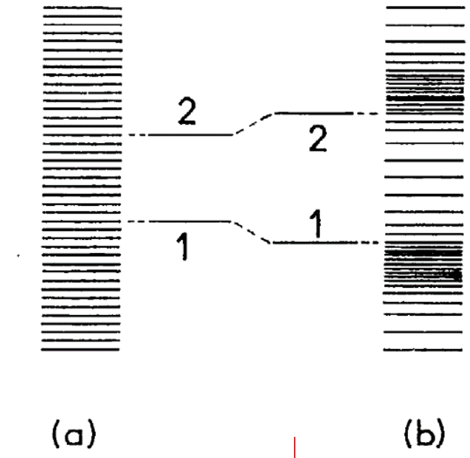

準位にギャップが開くと原子核が安定になる

$$E(\beta) = E_{LDM}(\beta) + E_{\rm shell}(\beta)$$

原子核が変形

→ 核子が感じるポテンシャルも変形

→ 変形度によって異なる量子力学的補正（殻効果）

殻構造の帰結：超重核の安定化

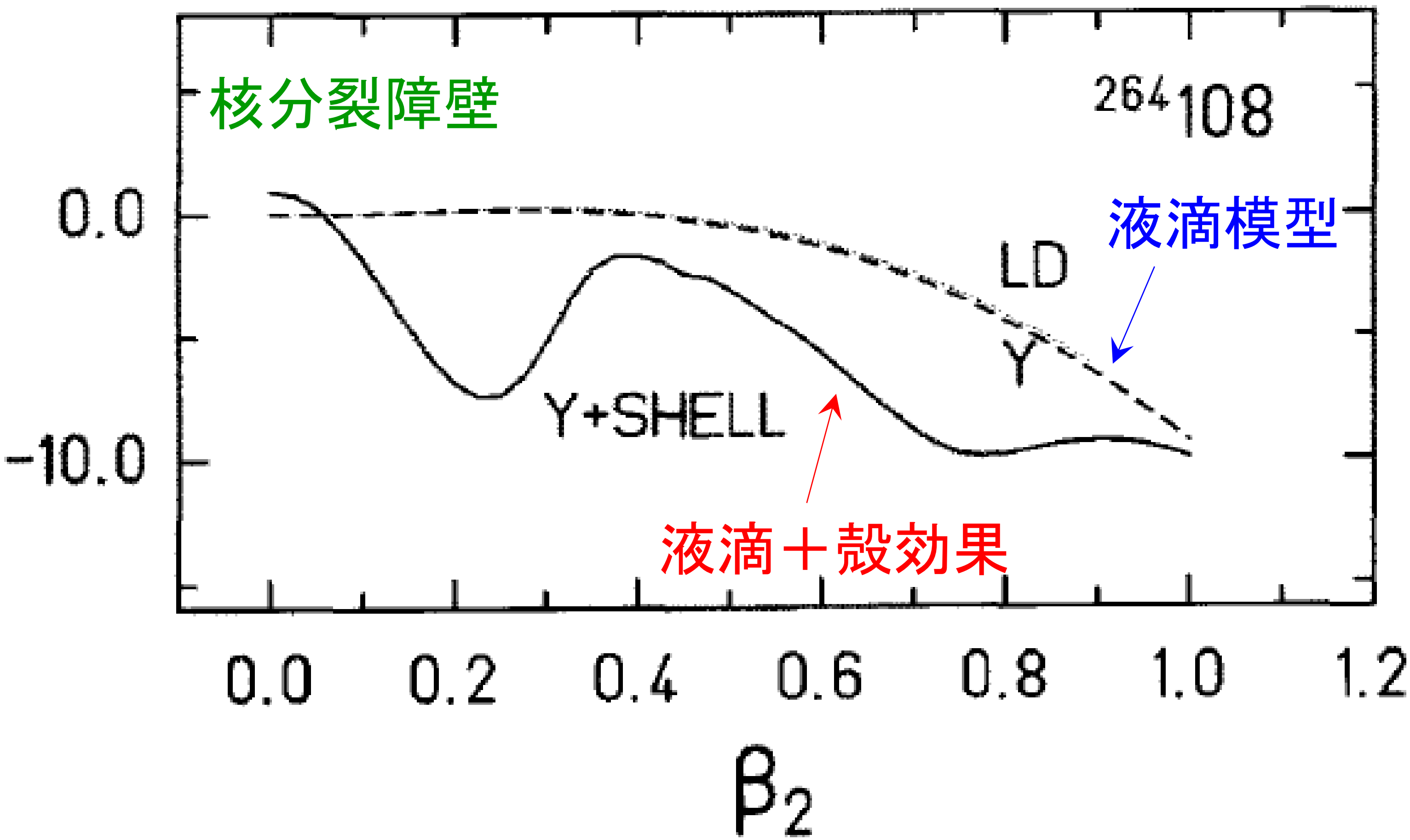

殻効果により核分裂障壁が高くなり原子核が安定化する

Z. Patyk et al., NPA491('89) 267

レポート問題6 PandAから提出、提出〆切　7/27（日）23:59

3次元非等方調和振動子

$$H = \frac{\boldsymbol{p}^2}{2m} + \frac{1}{2}m\omega_z^2 z^2 + \frac{1}{2}m\omega_\perp^2(x^2+y^2)$$

$$\begin{aligned}\omega_x = \omega_y \equiv \omega_\perp &= \omega_0\left(1+\frac{\epsilon}{3}\right)\\ \omega_z &= \omega_0\left(1-\frac{2}{3}\epsilon\right)\end{aligned}$$

を考える。ε を -1 から 1 まで変化させるとき、ε = 0 の時の基底状態、第一励起状態、第二励起状態のエネルギーはどのように変化するか図示せよ。

レポート問題7 PandAから提出、提出〆切　7/27（日）23:59

$E_0 = -\varepsilon$, $E_1 = \varepsilon$ のエネルギーをもつ2つの状態が強さ V で相互作用しているとする。このときの固有状態は 2x2行列

$$\begin{pmatrix} -\epsilon & V \\ V & \epsilon \end{pmatrix}$$

を対角化して得られる。2つの固有エネルギーの差が必ず 2ε (V=0のときのエネルギー差）より大きくなることを示せ。

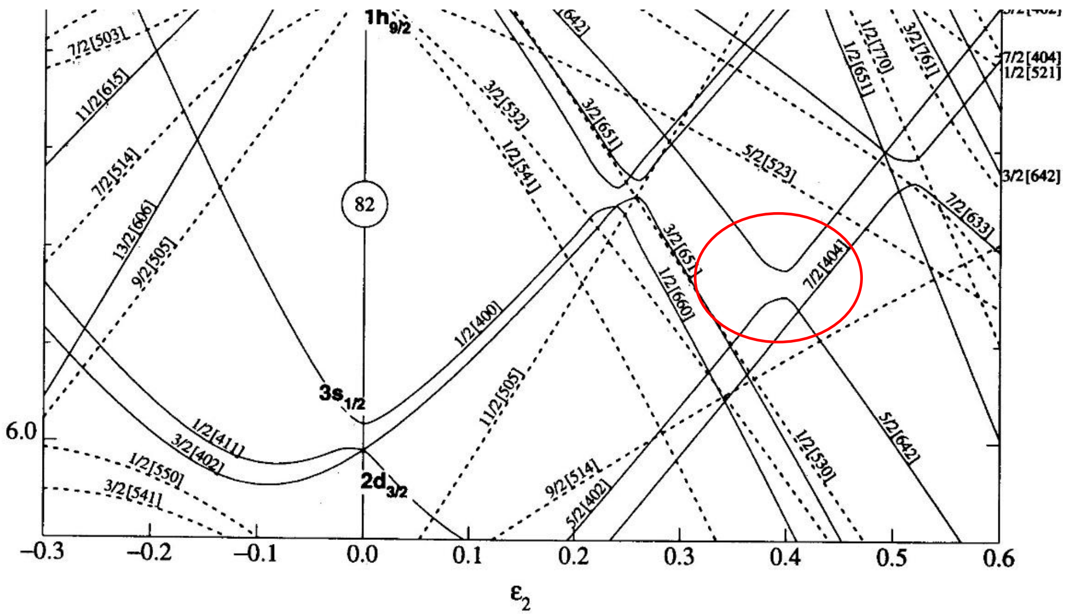

＊これを「ノイマン-ウィグナーの定理」といい、ニルソンレベルで準位反発が見られる理由である。

Angular Momentum Projection

- ✓ 変形→角運動量が混ざる（角運動量の固有状態になっていない）
- ✓ 観測される状態→角運動量の固有状態

$$
\begin{aligned}
H &= \sum_{i=1}^{A} -\frac{\hbar^2}{2m}\boldsymbol{\nabla}_i^2 + \frac{1}{2}\sum_{i,j}^{A} v(\boldsymbol{r}_i, \boldsymbol{r}_j) \\
&= \sum_{i=1}^{A} \left(-\frac{\hbar^2}{2m}\boldsymbol{\nabla}_i^2 + V_{\mathrm{MF}}(\boldsymbol{r}_i) \right) + \frac{1}{2}\sum_{i,j}^{A} v(\boldsymbol{r}_i, \boldsymbol{r}_j) - \sum_{i} V_{\mathrm{MF}}(\boldsymbol{r}_i)
\end{aligned}
$$

⇨ Ψ_{MF} : ハミルトニアン H が持っている対称性を持たなくてもいい

⇨ しかし、落とした項を考慮することによって
対称性を回復する必要がある

→角運動量射影

Angular Momentum Projection

- ✓ 変形→角運動量が混ざる（角運動量の固有状態になっていない）
- ✓ 観測される状態→角運動量の固有状態

→角運動量射影

0^+: no preference of direction (spherical)

⇒ Mixing of all orientations with an equal probability

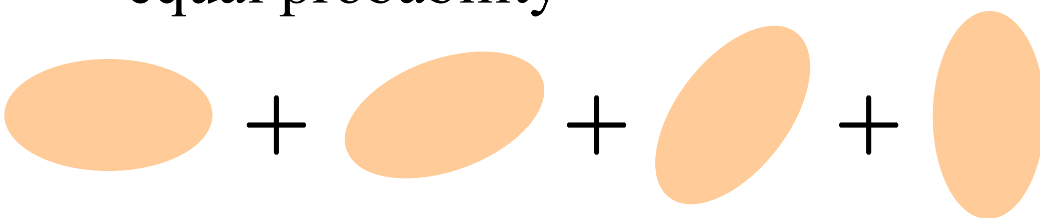

$$|\Psi_{0+}\rangle = \int d\Omega \, |\Psi_\Omega\rangle$$

other states:

$$|\Psi_{IM}\rangle = \int d\Omega \, Y_{IM}(\Omega) |\Psi_\Omega\rangle$$

(for K=0)

Projected wave function:

$$|\Psi_{IM}\rangle = \hat{P}^I_{MK}|\Psi\rangle = \frac{2I+1}{8\pi^2}\int d\Omega\, D^{I*}_{MK}(\Omega)\hat{\mathcal{R}}(\Omega)\,|\Psi\rangle$$

→ Projected energy surface:

$$E_I = \frac{\langle\Psi_{IM}|H|\Psi_{IM}\rangle}{\langle\Psi_{IM}|\Psi_{IM}\rangle} = \frac{\langle\Psi|\hat{P}^I_{KM}H\hat{P}^I_{MK}|\Psi\rangle}{\langle\Psi|\hat{P}^I_{KM}\,\hat{P}^I_{MK}|\Psi\rangle}$$

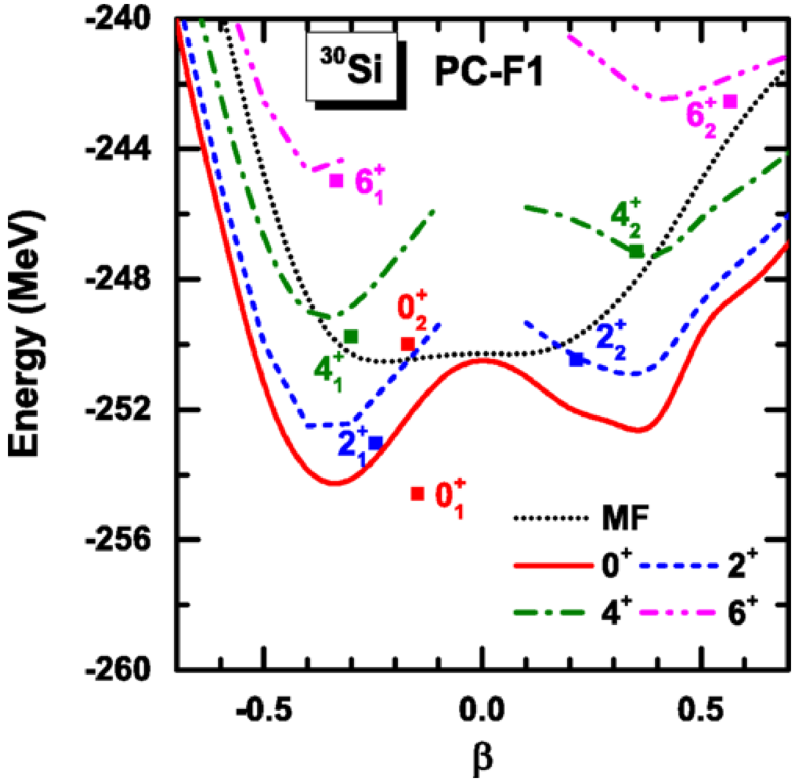

Constrained MF

0^+

2^+

4^+

H. Mei, K. Hagino, J.M. Yao,
T. Motoba, PRC97, 064318 (2018)

最近の話題

原子核の変形を核反応で視る

- ✓ 低エネルギー重イオン核融合反応
- ✓ 超高エネルギー重イオン衝突

Snapshots

taking snapshots of a "slow" motion with a high-speed camera

$$\tau_{\rm camera} \ll \tau_{\rm motion}$$

https://www.sony.jp/ichigan/products/ILCE-7M3/feature_3.html

(photos with a Sony camera α7III)

→ taking snapshots of a nucleus with a "fast" nuclear reaction

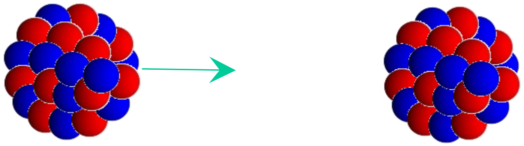

$$\tau_{\rm reaction} \ll \tau_{\rm nucleus}$$

Snapshots

taking a snapshot of a nucleus with a "fast" nuclear reaction

relativistic H.I. collisions
with a deformed nucleus

low-energy H.I. fusion reactions of a deformed nucleus

a good probe of
nuclear shapes

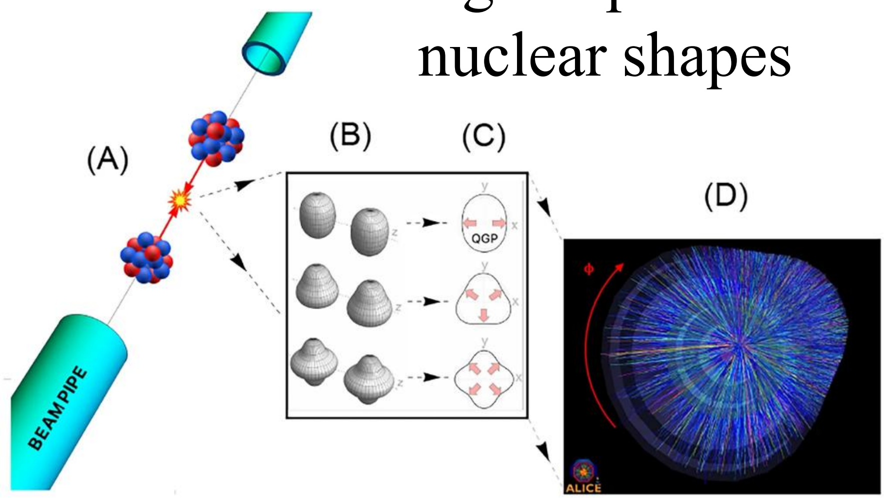

J. Jia et al.,
Nucl. Sci. Tech. 35, 220 (2024)

increasing interests
in recent years

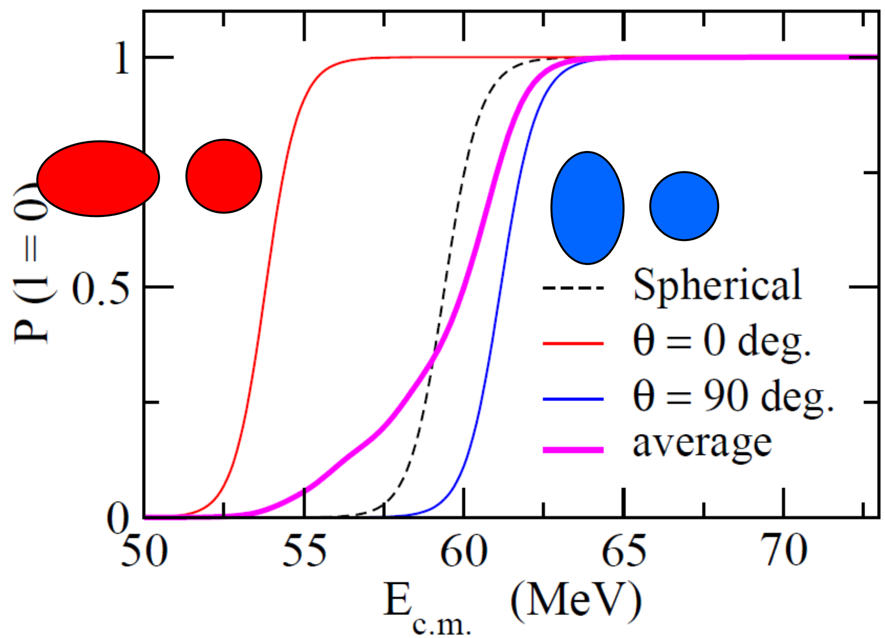

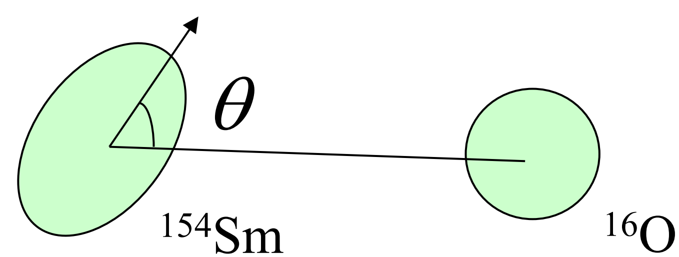

Snapshots

taking a snapshot of a nucleus with a "fast" nuclear reaction

relativistic H.I. collisions
with a deformed nucleus

low-energy H.I. fusion reactions of a deformed nucleus

a good probe of
nuclear shapes

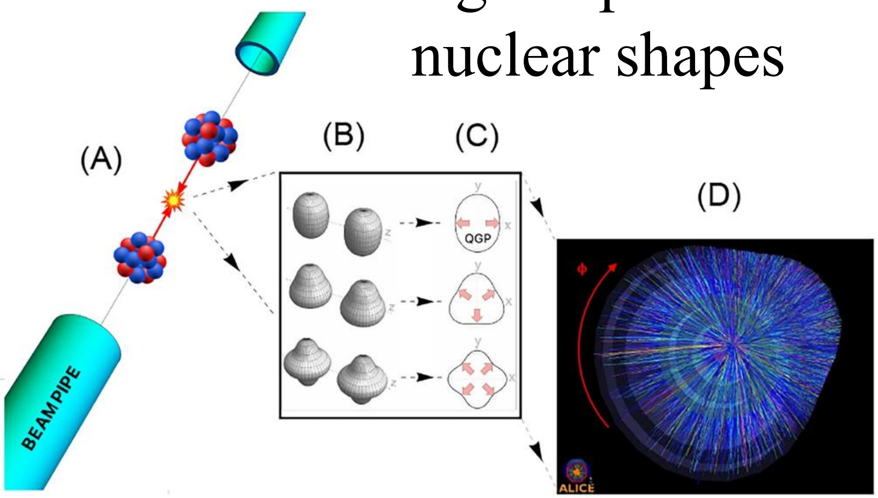

J. Jia et al.,
Nucl. Sci. Tech. 35, 220 (2024)

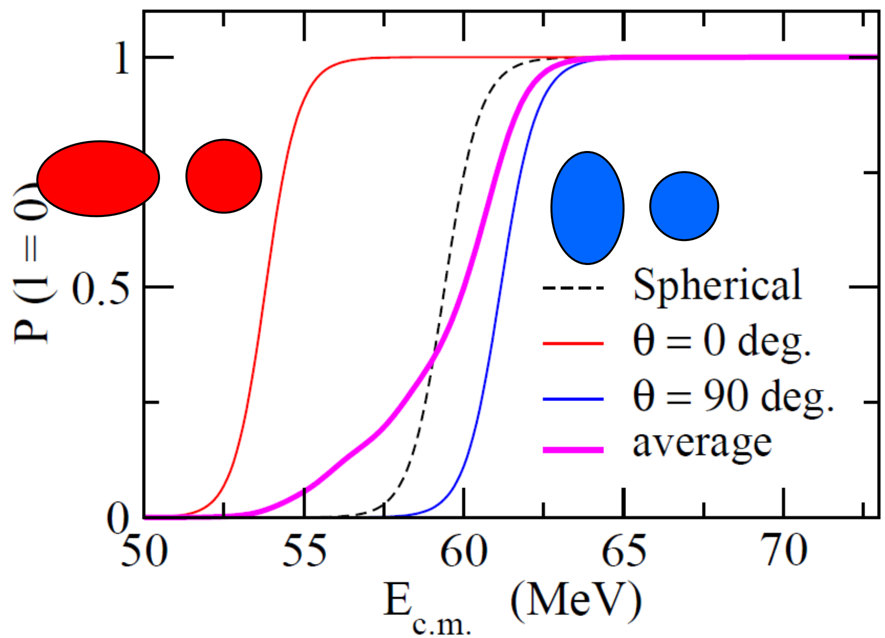

Large similarities: intersection of **High *E*** and **Low *E*** HI collisions

Low-energy heavy-ion fusion reactions

Coulomb barrier

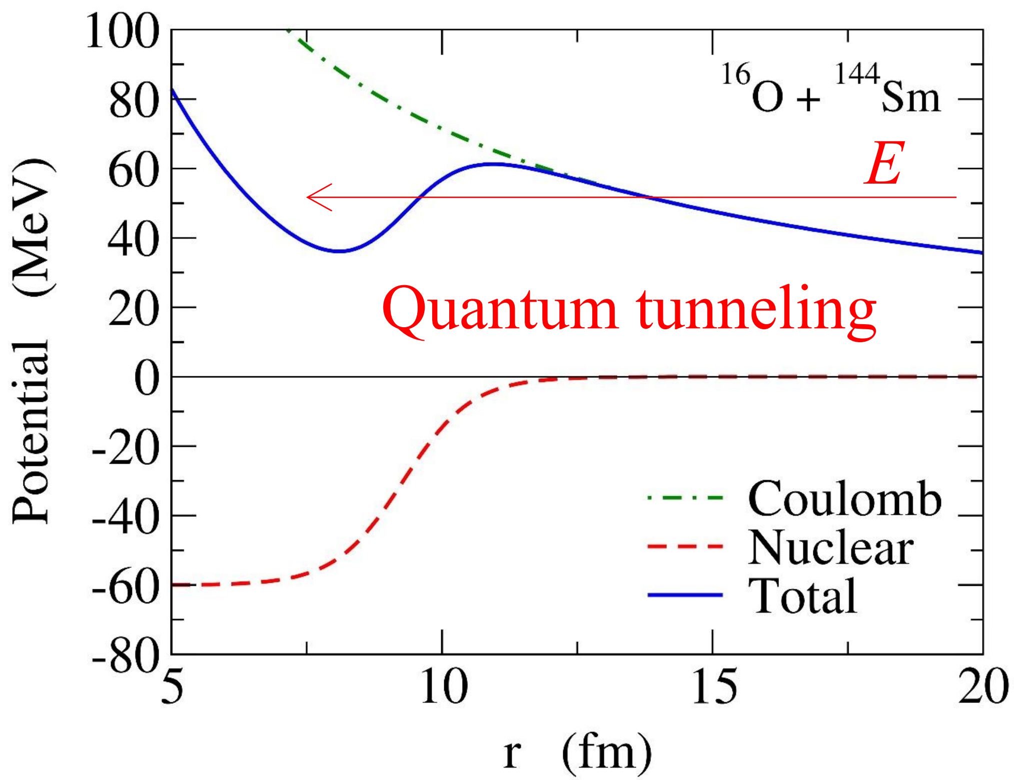

1. Coulomb interaction
   long range, repulsion
2. Nuclear interaction
   short range, attraction

↓

Potential barrier
(Coulomb barrier)

Fusion: takes place by overcoming the barrier

the barrier height → defines the energy scale of a system

Fusion reactions at energies around the Coulomb barrier

Low-energy heavy-ion fusion reactions and quantum tunneling

Fusion with quantum tunneling

with many degrees of freedom

- several nuclear shapes

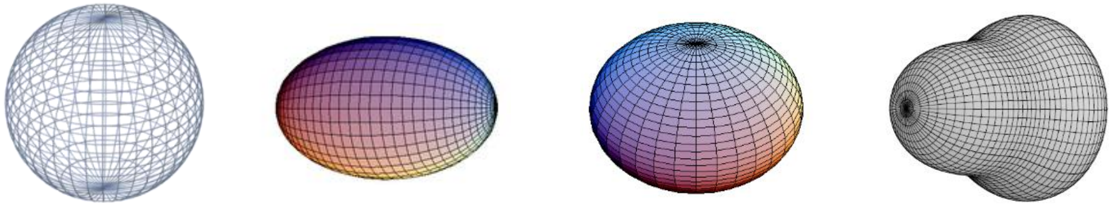

- several surface vibrations

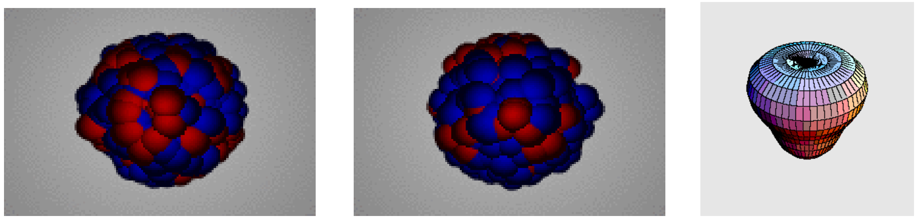

https://web-docs.gsi.de/~wolle/TELEKOLLEG/KERN/index-s.html

several modes and adiabaticities

- several types of nucleon transfers

Tunneling probabilities: the exponential E dependence
→ (small) nuclear structure effects are **amplified**

Discovery of large sub-barrier enhancement of σ_{fus} (~80's)

the potential model: inert nuclei (no structure)

$$\sigma_{\text{fus}} = \frac{\pi}{k^2}\sum_l (2l+1)(1-|S_l|^2)$$

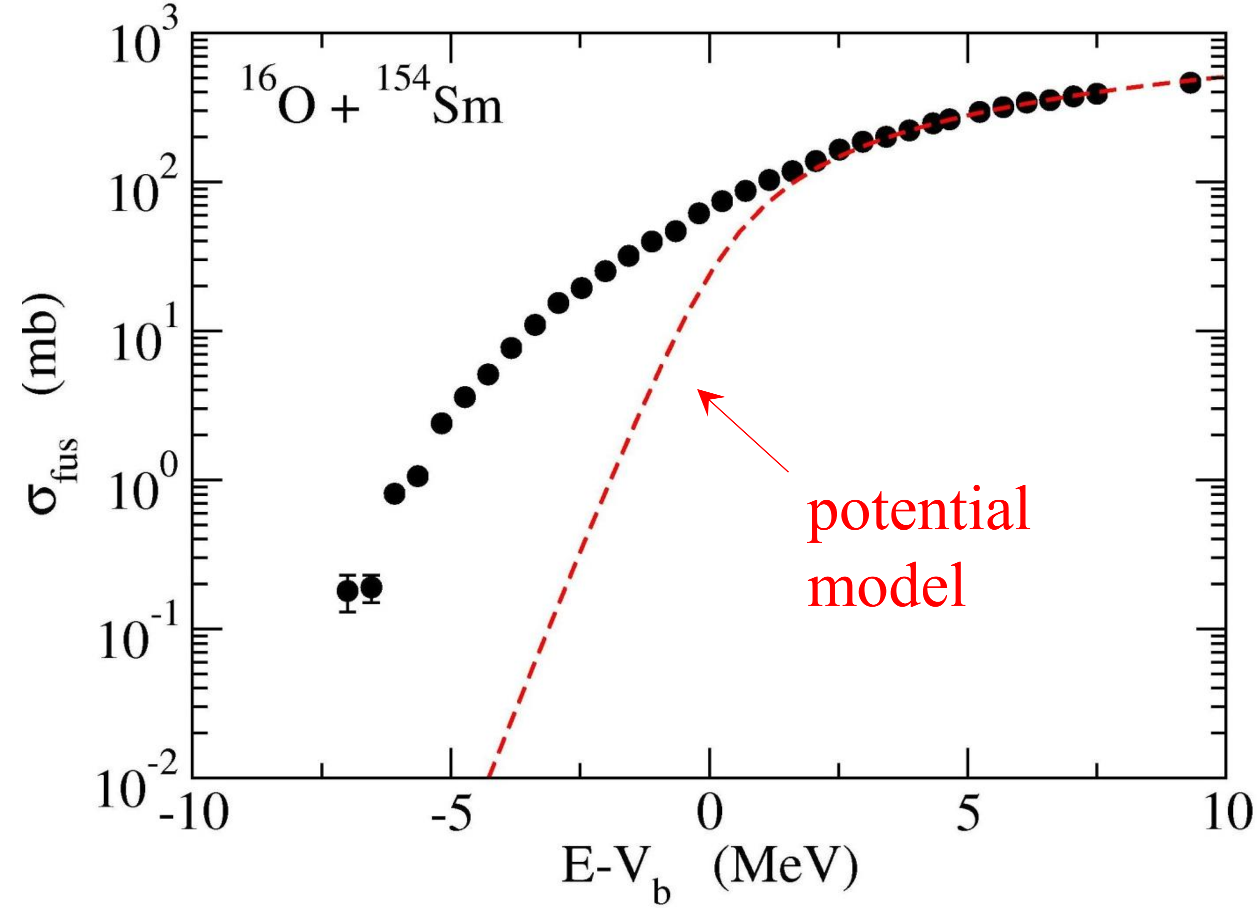

^{154}Sm : a typical deformed nucleus

$$E_I \sim \frac{I(I+1)\hbar^2}{2\mathcal{J}}$$

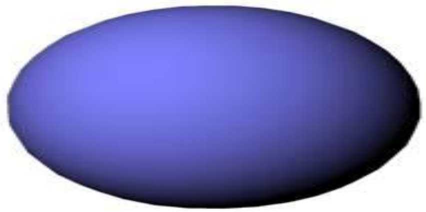

^{154}Sm

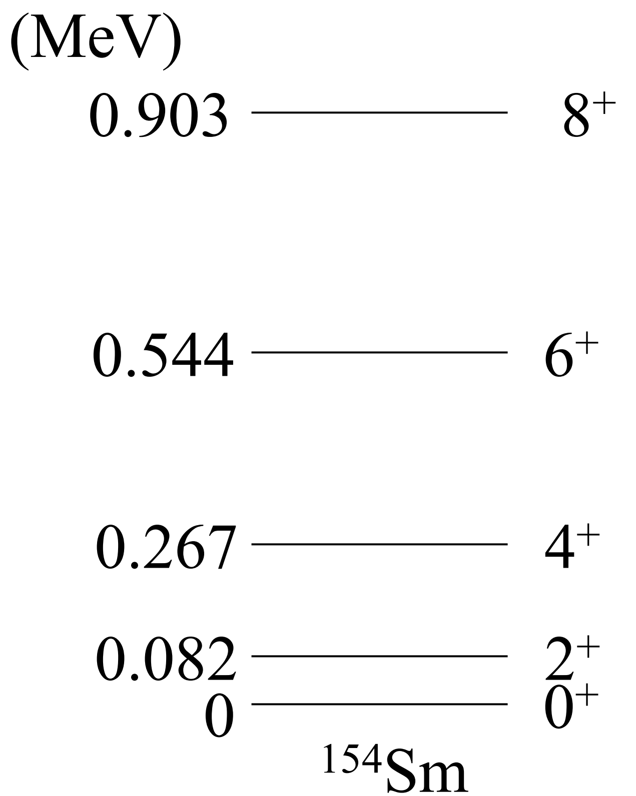

rotational spectrum

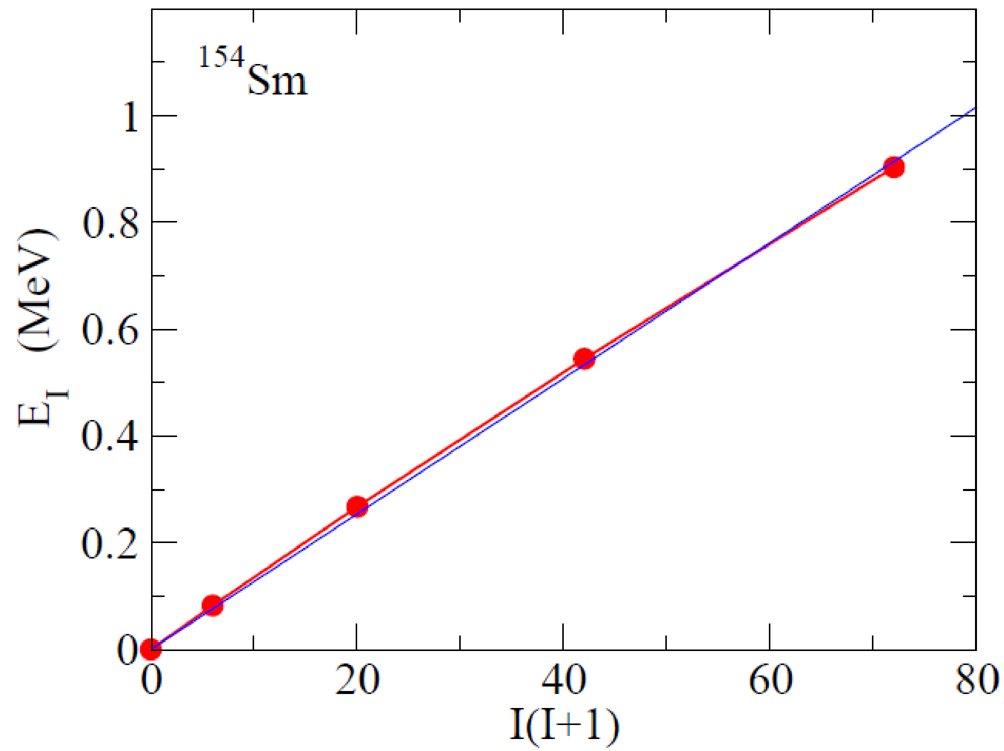

cf. a classical rigid rotor

$$E = \frac{1}{2}\mathcal{J}\omega^2 = \frac{I^2}{2\mathcal{J}}$$

$$(I = \mathcal{J}\omega,\ \ \omega = \dot{\theta})$$

Effects of nuclear deformation

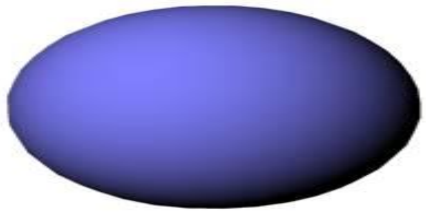

^{154}Sm

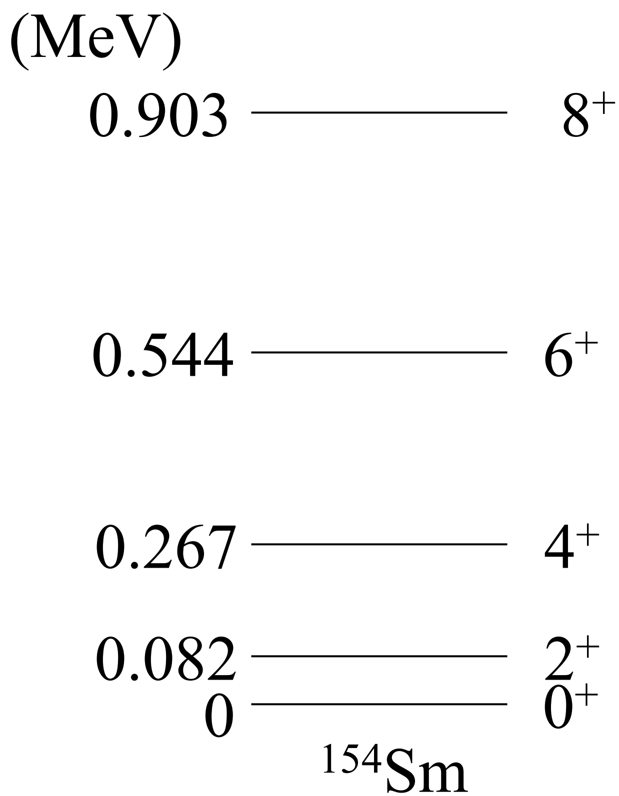

rotational spectrum

a small rotational energy

$$E_I = \frac{I(I+1)\hbar^2}{2\mathcal{J}}$$

→ a large moment of inertia J

→ rotation: a slow deg. of freedom

$$E_{\rm rot} \sim E_{2^+} = 82 \text{ keV}$$
$$E_{\rm tunnel} \sim \hbar\Omega_{\rm barrier} \sim 3.5 \text{ MeV}$$

$\Psi_{0^+} =$ 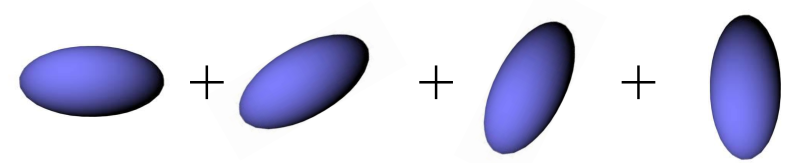

→ a spherical state
in the lab. system

fix the orientation angle to calculate
the fusion probability

"a snapshot of a rotating nucleus"

^{154}Sm : a typical deformed nucleus

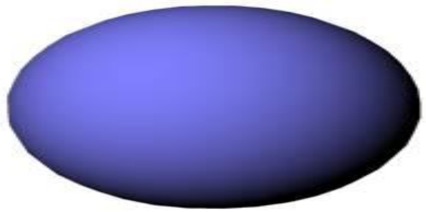

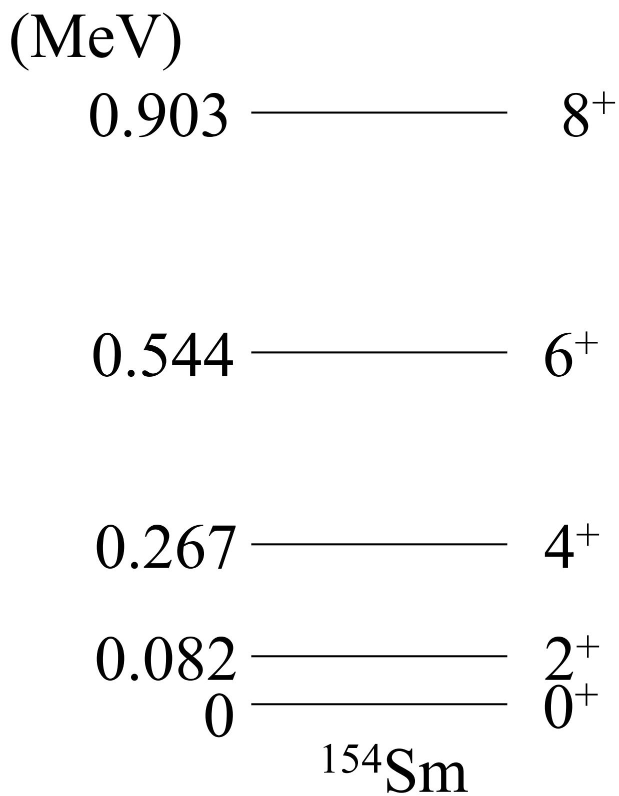

rotational spectrum

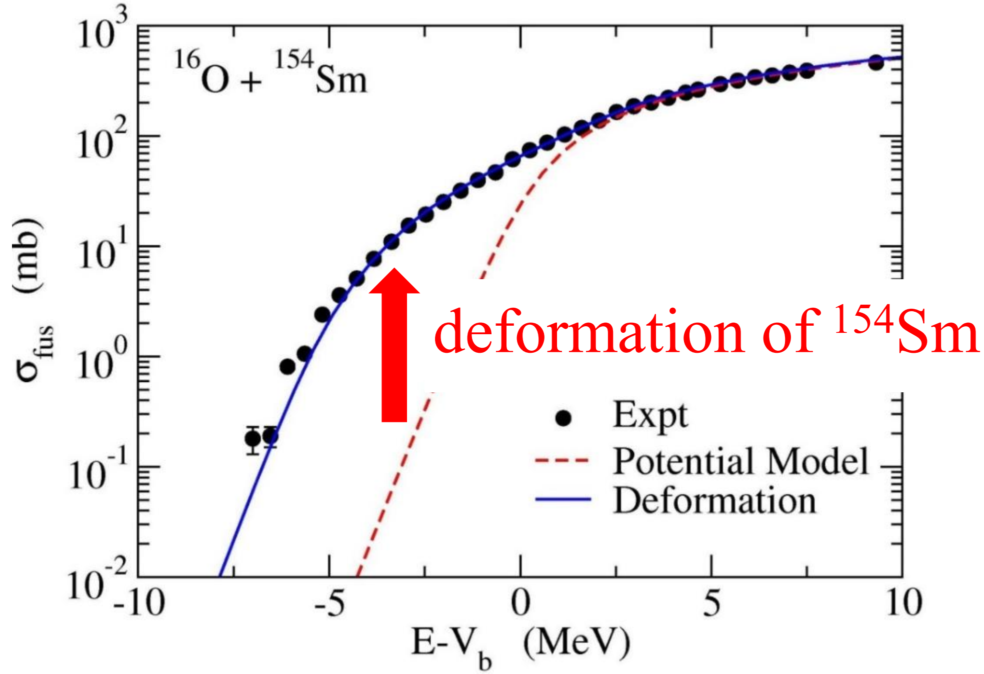

K. H. and N. Takigawa,
Prog. Theo. Phys.128 ('12)1061.

$$\sigma_{\text{fus}}(E) = \int_0^1 d(\cos\theta)\sigma_{\text{fus}}(E;\theta)$$

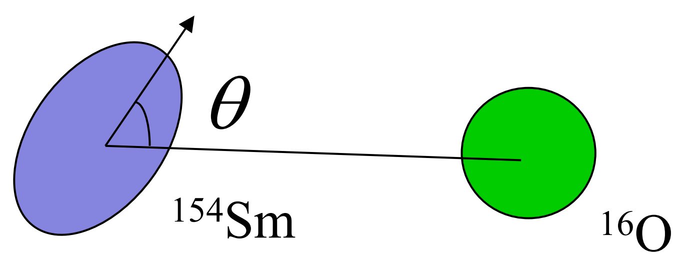

Effects of nuclear deformation

^{154}Sm : a typical deformed nucleus

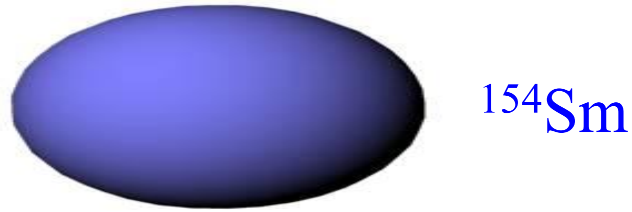

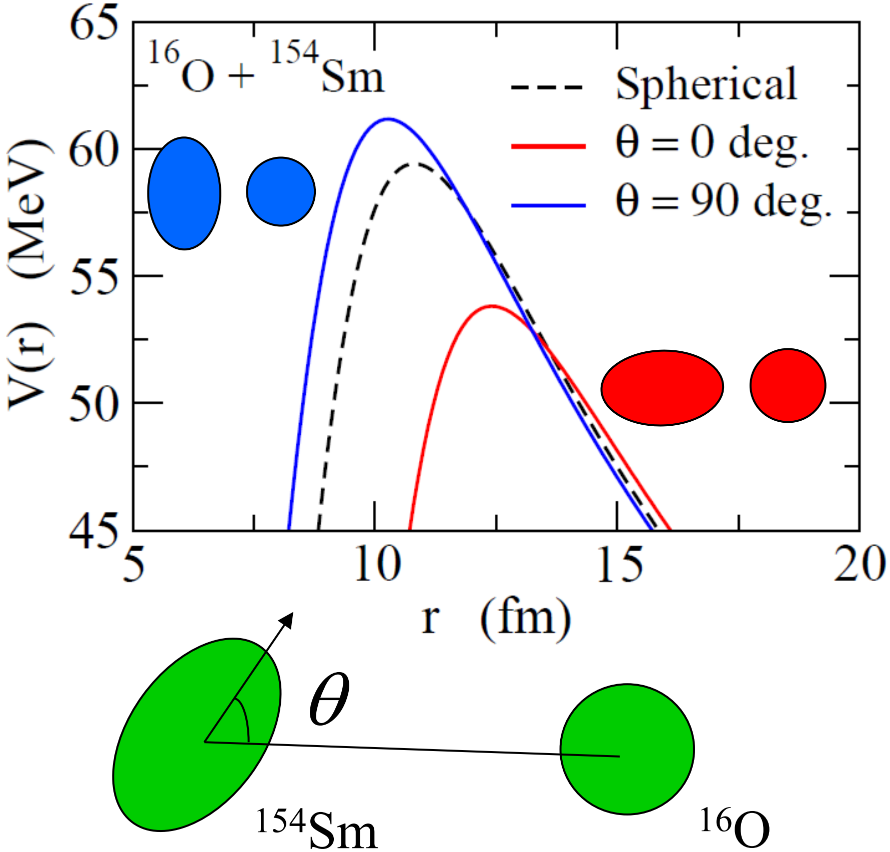

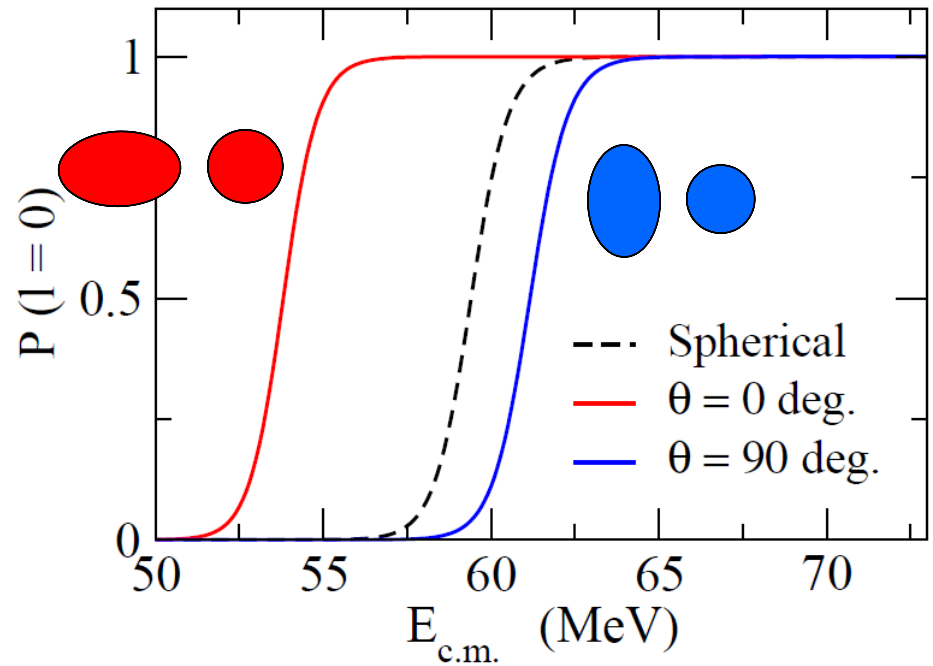

Effects of nuclear deformation

^{154}Sm : a typical deformed nucleus

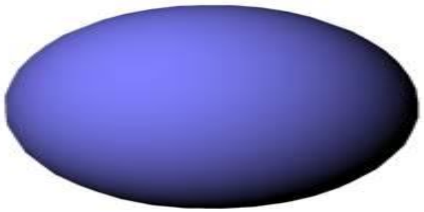

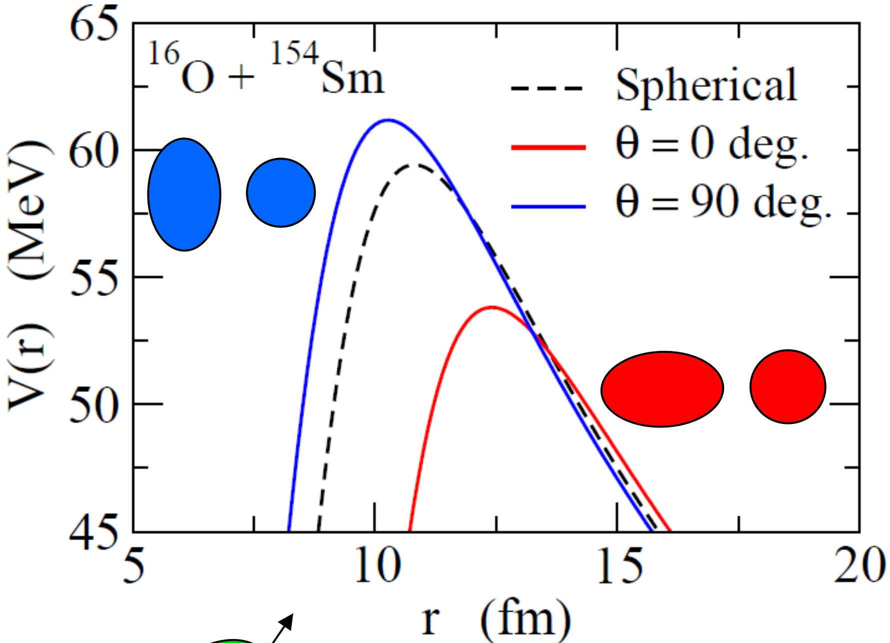

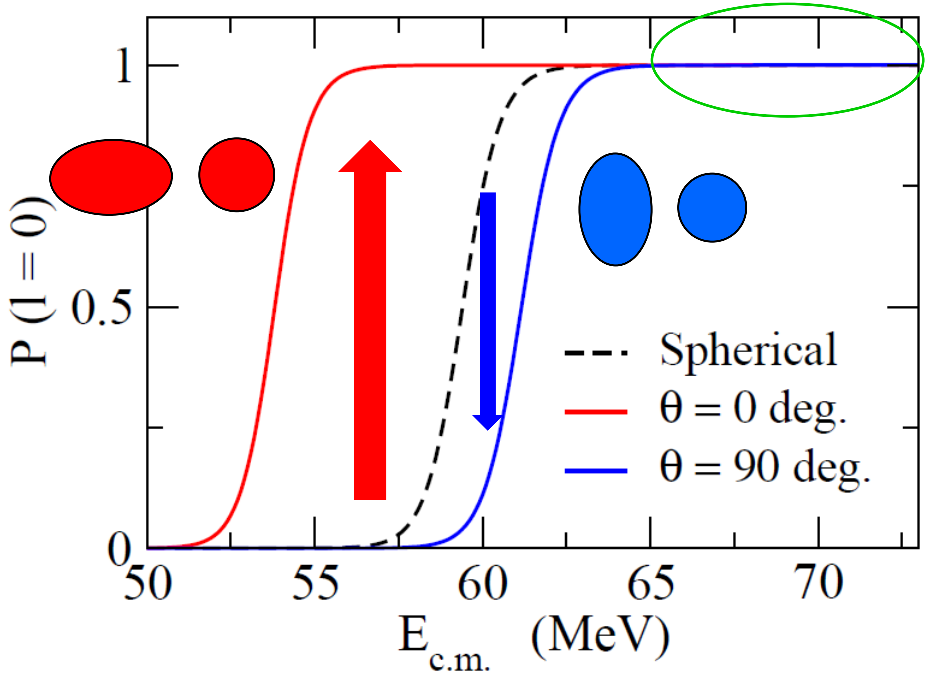

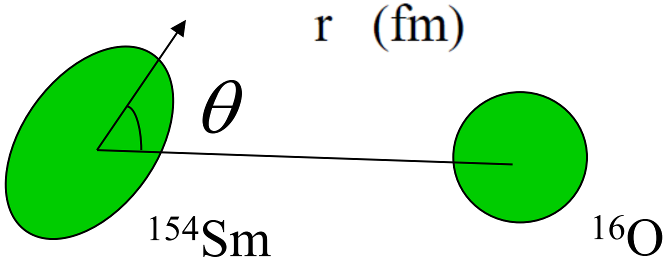

Effects of nuclear deformation

^{154}Sm : a typical deformed nucleus

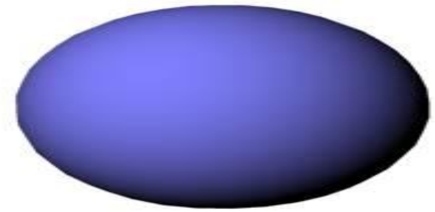

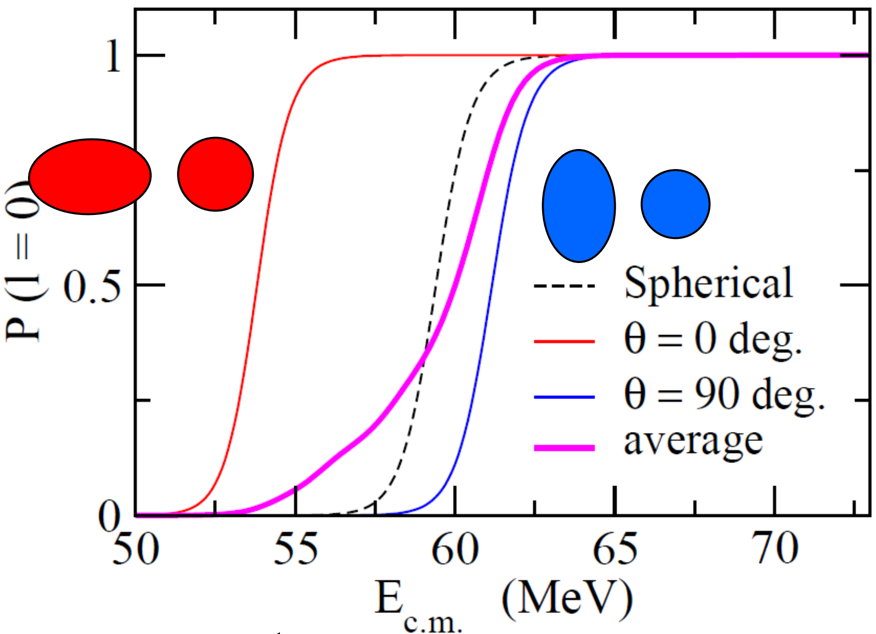

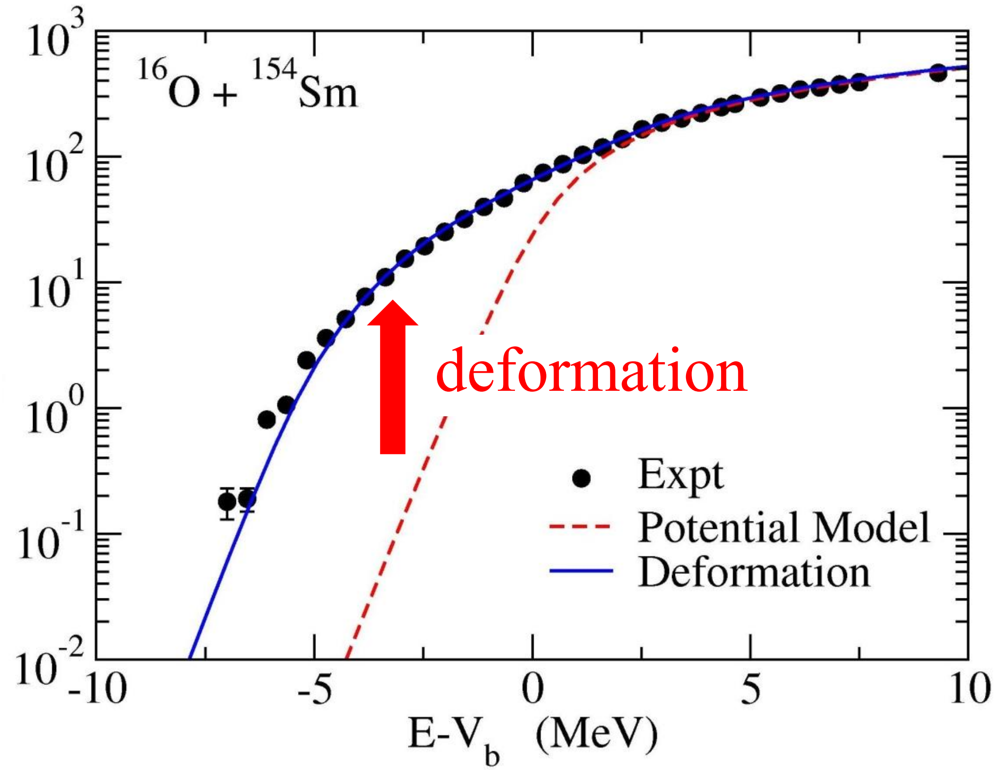

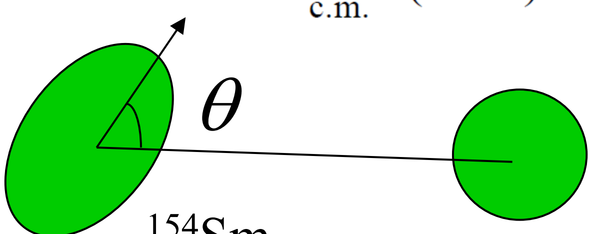

$$\sigma_{\text{fus}}(E) = \int_0^1 d(\cos\theta)\sigma_{\text{fus}}(E;\theta)$$

Fusion: strong interplay between nuclear structure and reaction

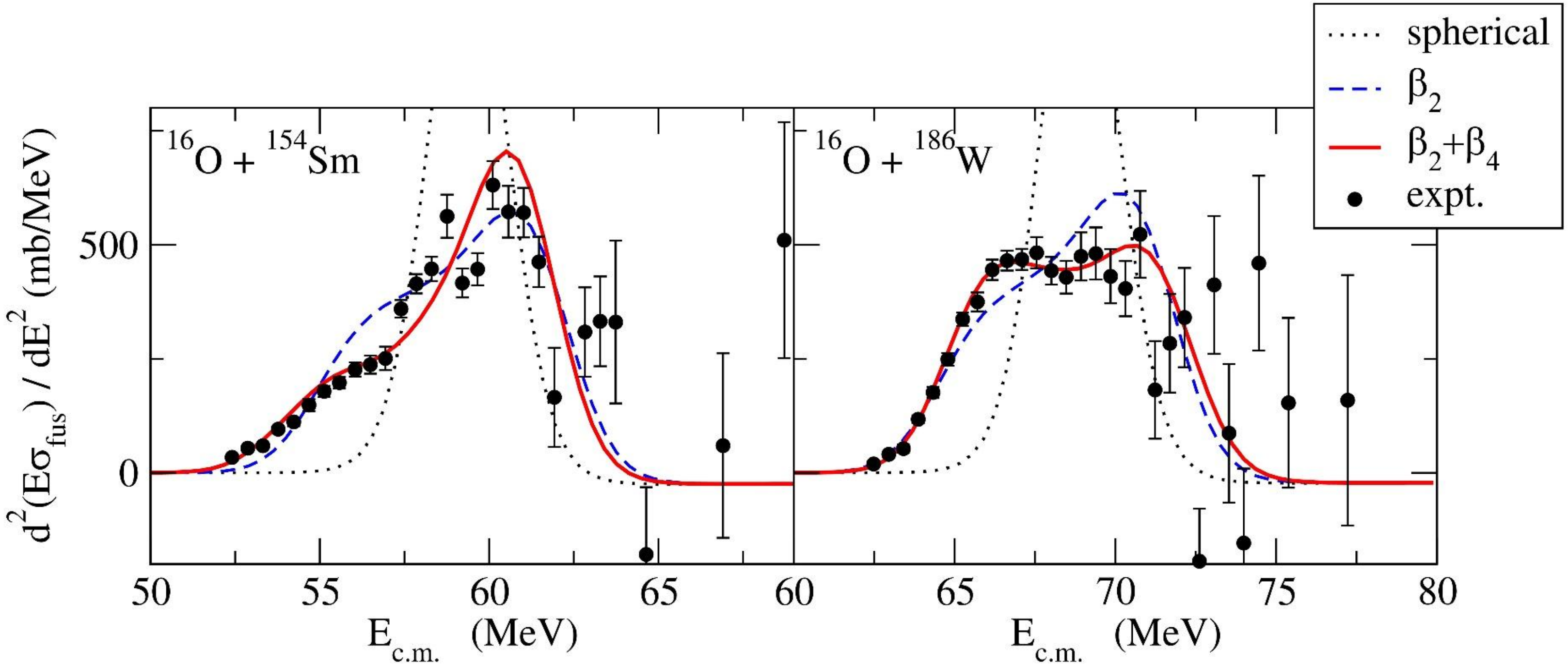

$$R(\theta) = R_0(1 + \beta_2 Y_{20}(\theta) + \beta_4 Y_{40}(\theta) + \cdots)$$

$\beta_2 = 0.33$

$\beta_4 = +0.05$

$\beta_2 = 0.29$

$\beta_4 = -0.03$

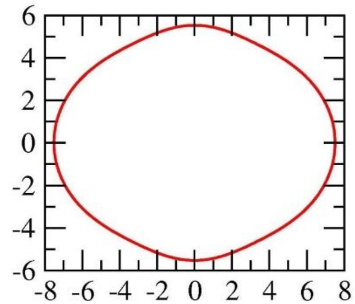

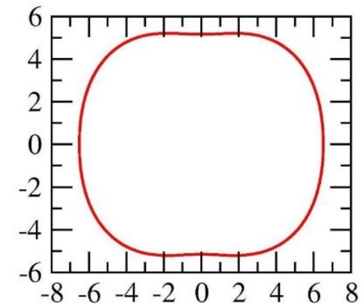

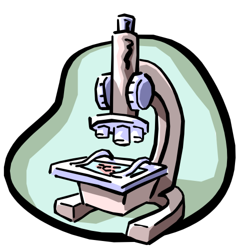

sensitive to the sign of β_4!

→ Fusion as a quantum tunneling microscope for nuclei

Probing nuclear shapes in Rel. H.I. collisions

the initial shape of QGP **expansion** **detection**

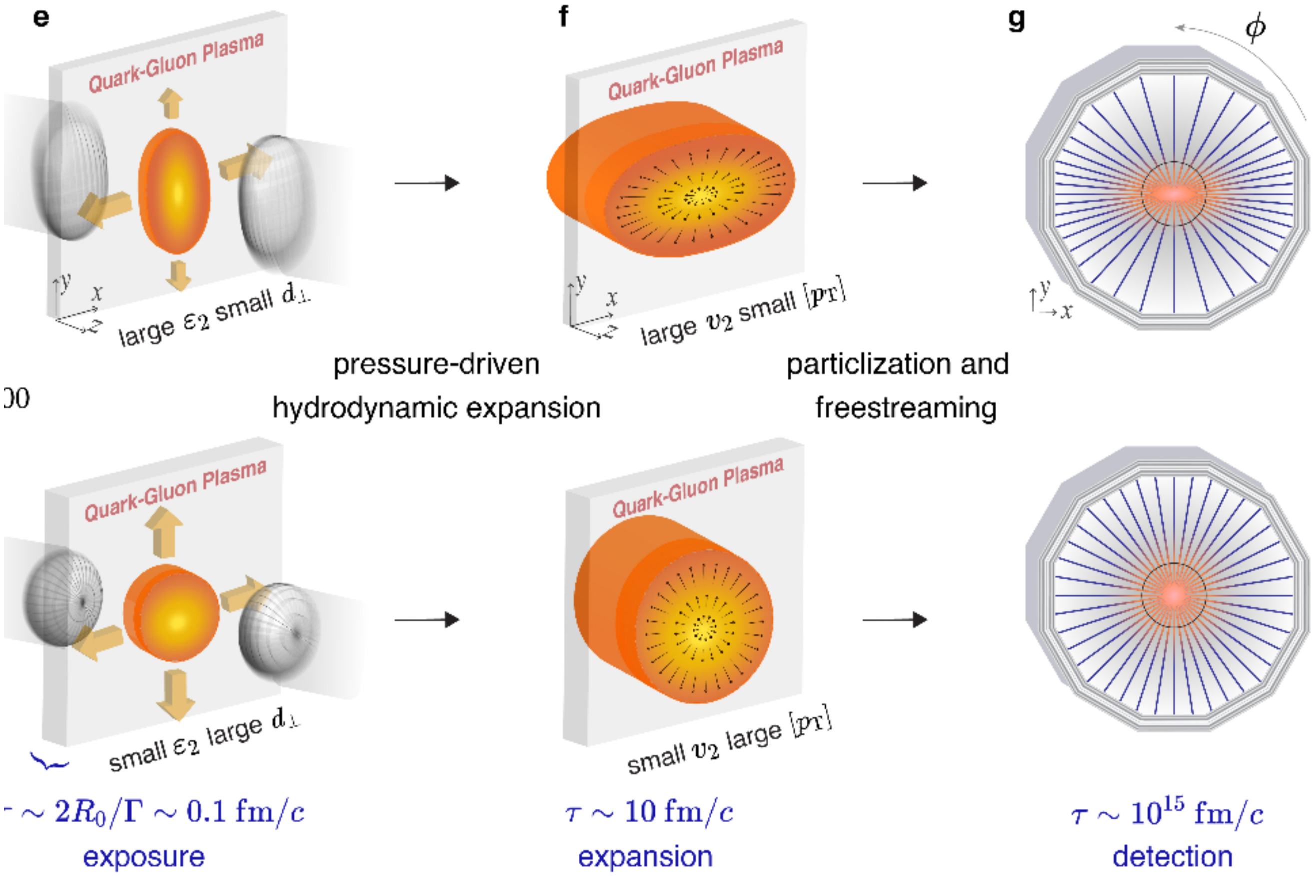

M.I. Abdulhamid et al. (STAR collaboration)
Nature 635, 67 (2024)

Probing nuclear shapes in Rel. H.I. collisions

flow:
the final N-distribution

$$\frac{1}{N}\frac{dN}{d\phi} = \frac{1}{2\pi}\left[1 + 2\sum_n v_n \cos n(\phi - \Psi_n)\right]$$

elliptic（楕円）flow v_2

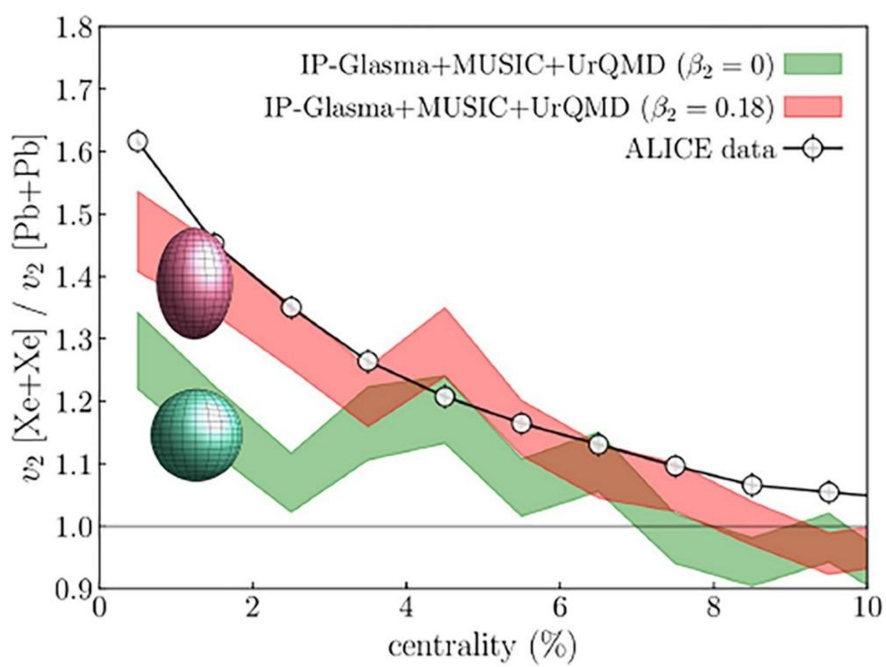

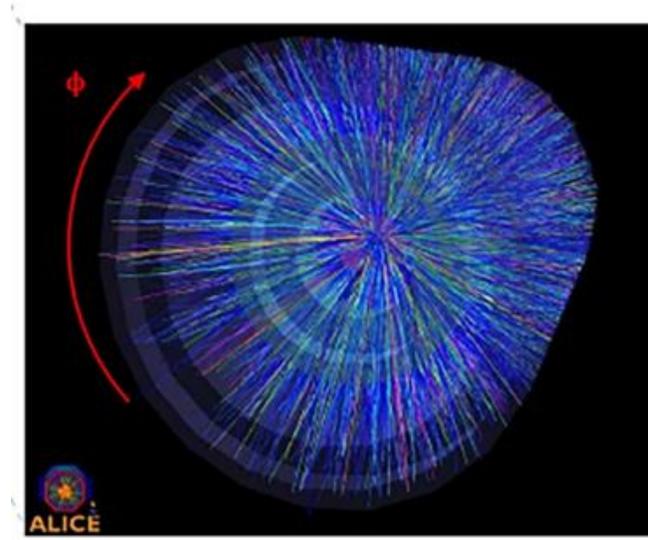

the ratio of ^{129}Xe+^{129}Xe to ^{208}Pb+^{208}Pb
→ quadrupole deformation of ^{129}Xe

J. Jia et al.,
Nucl. Sci. Tech. 35, 220 (2024)

Probing nuclear shapes in Rel. H.I. collisions

flow:
the final N-distribution

$$\frac{1}{N}\frac{dN}{d\phi} = \frac{1}{2\pi}\left[1 + 2\sum_n v_n \cos n(\phi - \Psi_n)\right]$$

elliptic（楕円）flow v_2

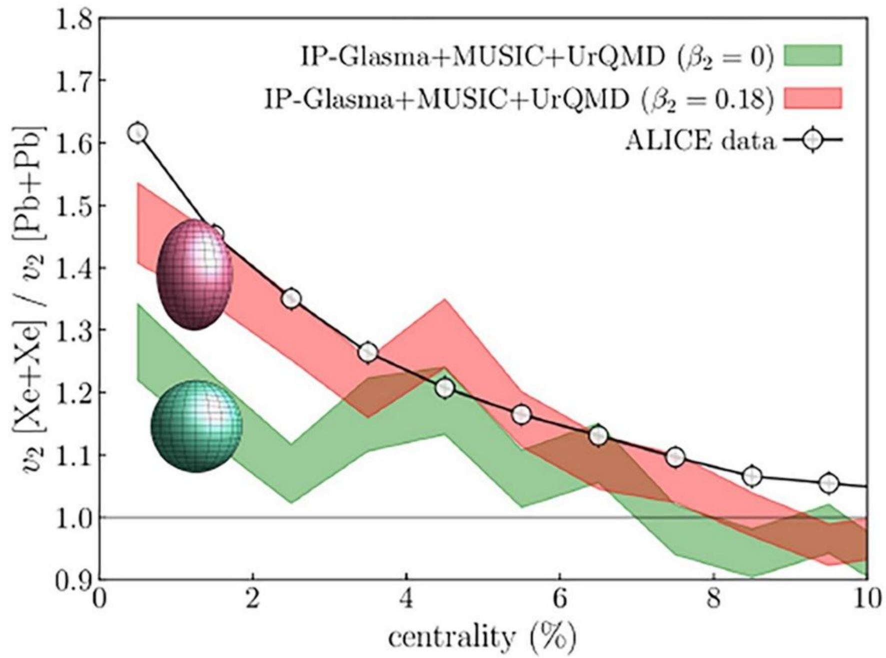

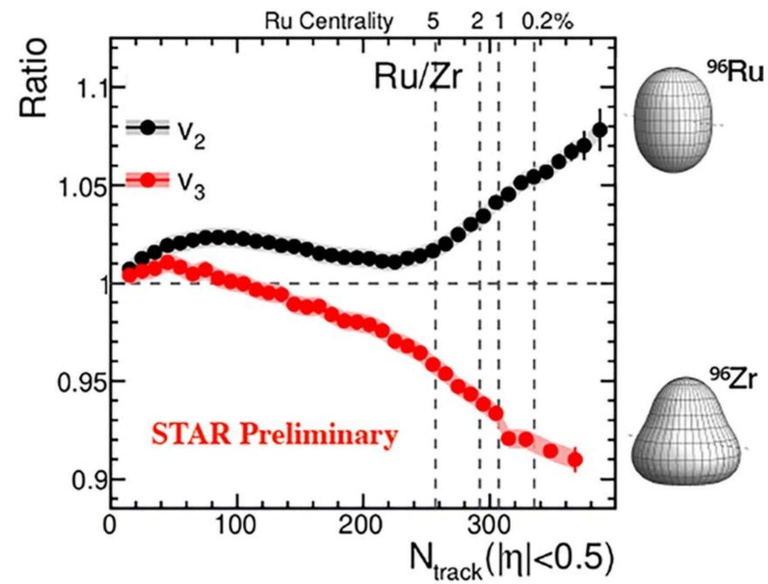

the ratio of ^{96}Ru+^{96}Ru to ^{96}Zr+^{96}Zr
→ octupole deformation of ^{96}Zr

the ratio of ^{129}Xe+^{129}Xe to ^{208}Pb+^{208}Pb
→ quadrupole deformation of ^{129}Xe

J. Jia et al.,
Nucl. Sci. Tech. 35, 220 (2024)

Probing nuclear shapes in Rel. H.I. collisions

flow:
the final N-distribution

$$\frac{1}{N}\frac{dN}{d\phi} = \frac{1}{2\pi}\left[1 + 2\sum_n v_n \cos n(\phi - \Psi_n)\right]$$

other examples:

✓ triaxial (γ) deformation



- G. Aad et al., PRC107, 054910 (2023)
- STAR collaboration, Nature 635, 67 (2024)

✓ α cluster

- $^{16}O+^{16}O$: ALICE, preliminary
- Y. Wang et al., PRC109, L051904 (2024)

NLEFT

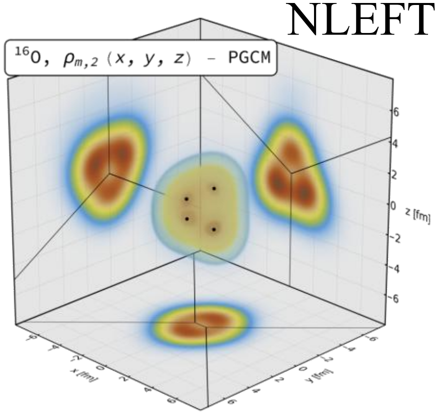

G. Giacalone et al., arXiv: 2402.05995